

**Permafrost-Controlled Break in Fractal Scaling of River Networks, Yukon Coastal Plain,
Western Canadian Arctic**

Adam S. Mawer

Department of Earth Sciences, Dalhousie University, Halifax, Nova Scotia, Canada. B3h 3J5

Keywords: Arctic River Networks, Permafrost, Peat, Fractal, Horton Ratios

**Permafrost-Controlled Break in Fractal Scaling of River Networks, Yukon Coastal Plain,
Western Canadian Arctic**

Adam S. Mawer

Department of Earth Sciences, Dalhousie University, Halifax, Nova Scotia, Canada. B3h 3J5

Submitted in partial fulfillment for a Bachelor of
Science Honours Degree, Dalhousie University, Halifax, Nova Scotia
March 28, 2005



Dalhousie University

Department of Earth Sciences

Halifax, Nova Scotia

Canada B3H 3J5

(902) 494-2358

FAX (902) 494-6889

DATE: April 29, 2005

AUTHOR: Adam S. Mawer

TITLE: "Permafrost-Controlled Break in Fractal
Scaling of River Networks, Yukon Coastal
Plain, Western Canadian Arctic"

Degree: B.Sc. (Hons) Convocation: May 25 Year: 2005

Permission is herewith granted to Dalhousie University to circulate and to have copied for non-commercial purposes, at its discretion, the above title upon the request of individuals or institutions.

THE AUTHOR RESERVES OTHER PUBLICATION RIGHTS, AND NEITHER THE THESIS NOR EXTENSIVE EXTRACTS FROM IT MAY BE PRINTED OR OTHERWISE REPRODUCED WITHOUT THE AUTHOR'S WRITTEN PERMISSION.

THE AUTHOR ATTESTS THAT PERMISSION HAS BEEN OBTAINED FOR THE USE OF ANY COPYRIGHTED MATERIAL APPEARING IN THIS THESIS (OTHER THAN BRIEF EXCERPTS REQUIRING ONLY PROPER ACKNOWLEDGEMENT IN SCHOLARLY WRITING) AND THAT ALL SUCH USE IS CLEARLY ACKNOWLEDGED.

Abstract

River networks have been proposed to be scale-invariant patterns characterized by approximately constant bifurcation, length, and area ratios across all stream orders. Moreover, the ratios appear to vary over a relatively small range across a wide range of geology, climate, and relief. However, Arctic river networks remain a poorly examined facet of fluvial geomorphology. First order, qualitative observations suggest processes are significantly different than temperate networks. For example, dominant discharges may be thaw lake floods, not freshets, and many hillslopes appear to be drained by highly channelized flow through 1-10 m wide linear regions of porous peat, referred to as water tracks. To investigate scaling behaviour, and underlying physical processes, in Arctic networks, I compare Hortonian classification and laws of drainage networks in the Yukon coastal plain with lower latitude networks including the Peace River hills of Northern Alberta, the Okanagan Valley of south central British Columbia, and the coastal plains of eastern Nova Scotia. Comparisons use channel networks extracted from DEM, tested against aerial photographs. Water tracks have a critical basin area of $0.10 \pm 0.09 \text{ km}^2$, whereas open water channels form where basin areas exceed $11.0 \pm 9.67 \text{ km}^2$ in the Running River basin. Ratios in Arctic networks are atypically not uniform across different channel orders with jumps in bifurcation (4.6 to 3.0), length (1.7 to 1.1), area (4.5 to 3.5) and gradient (1.2 to 1.3) ratios from the third to fourth order respectively. High bifurcation ratios of low order streams, depressed length ratios, and similar area ratios of high latitude (Arctic) networks are a hydrological response to frozen, impermeable permafrost, and coherent fibric peat which resists channelization. At lower latitudes, channels also originate as focused flows (rills) that incise and cross grade owing to erodible substrate, not cemented by permafrost, eventually evolving into numerous incised channels. Fibric peat in permafrost regions further resists channelization owing to hydraulic conductivity 10 times higher than typical soils, which prevents erosive overland flow. Under current and anticipated degradation of permafrost by anthropogenic warming, incision of water tracks into low order streams may force Arctic drainage networks to mirror their lower latitude counterparts and obey fractal classifications.

Table of Contents	Page
Abstract.....	i
Table of Contents.....	ii
List of Figures.....	iv
List of Tables.....	vi
List of Variables.....	vii
Acknowledgements.....	viii
 Chapter 1.0.0: Introduction	
1.1.0: Statement of the Problem.....	1
1.2.0: Study Area.....	2
1.3.0: Previous Work.....	3
1.4.0: Significance.....	4
 Chapter 2.0.0: Network Classification and River Morphology	
2.1.0: General Background.....	6
2.2.0: Fractal Classification.....	7
2.3.0: Network Properties.....	7
2.4.0: Graphical Representation of Hortons Laws for Measured Networks.....	10
2.5.0: Hortonian Qualitative Erosional Evolution of Streams.....	12
2.6.0: Alluvial and Fluvial River Processes.....	14
 Chapter 3.0.0: Arctic Peat, Permafrost and Rivers	
3.1.0: General Background.....	16
3.2.0: Permafrost Categorization.....	16
3.2.1: Hydraulic Properties of Permafrost.....	19
3.3.0: Peat.....	21
3.3.1: Peat as an Insulator.....	21
3.3.2: Hydraulic Properties of Peat.....	22
3.4.0: Arctic Rivers.....	23
3.5.0: Thaw Lake and Thermokarst Topography.....	24
 Chapter 4.0.0: Field Locations	
4.1.0: Yukon Coastal Plain.....	26
4.2.0: Bedrock Geology.....	27
4.3.0: Quaternary Geology.....	31
4.4.0: Quaternary Climate.....	33
4.5.0: Recent Climate.....	35
4.6.0: Temperate Study locations.....	38
 Chapter 5.0.0: Methods	
5.1.0: General Approach.....	40

5.2.0: Digital Elevation Models (DEMs).....	40
5.2.1: Digital Elevation Model Acquisition.....	41
5.3.0: Drainage Network Analysis.....	42
5.4.0: Air Photo Inspection.....	43
Chapter 6.0.0: Results and Discussion	
6.1.0: Bifurcation (R_B), Area (R_A), Length (R_L), and Channel Gradient (R_G)	
Ratios in the Running River Drainage Basin.....	45
6.1.1: All Channels.....	46
6.1.2: Channels Below Order 3.....	47
6.1.3: Open Water Channels.....	48
6.1.4: Comparison with Temperate Networks.....	49
6.2.0: Critical Basin Areas.....	52
6.3.0: Discussion.....	52
6.3.1: Causes of Open Water Channels on the Yukon Coastal Plain.....	56
6.3.2: Effects of Anthropogenic Global Warming.....	57
Chapter 7.0.0: Conclusion.....	58
References.....	61
Appendix A: Quaternary Geology of the Yukon Coastal Plain.....	66
Appendix B: Digital Elevation Model MetaData.....	68
Appendix C: Aerial Photographs and Attributes.....	70
Appendix D: Horton Plots for all Study Areas.....	76
Appendix E: Calculations.....	80

List of Figures

	Page
Figure 1.1: Study site location on the Yukon Coastal Plain in the Western Canadian Arctic.....	2
Figure 1.2: Contoured map (10 meter intervals) of the Yukon Coastal Plains' topography in the area of my study site.....	3
Figure 1.3: Change in near surface temperature from 1900-2004.....	4
Figure 2.1: River network illustrating Horton-Strahler stream ordering.....	6
Figure 2.2: Fractal classification in nature.....	7
Figure 2.3: River network branching scheme illustrating nature's self-affine properties in fractal classification.....	8
Figure 2.4: Graphical representation of the Mamon river basin showing approximate linear nature of plots and derived Hortonian laws	11
Figure 2.5: River valley incision in the Keg River region (AB) operating in accordance with Hortonian incision.....	14
Figure 3.1: Global distribution of permafrost.....	16
Figure 3.2: Continuous permafrost distribution in Canada.....	17
Figure 3.3: Talik types and geometry within permafrost.....	18
Figure 3.4: Hydraulic conductivity of different types of frozen soils as a function of temperature.....	19
Figure 3.5: Fibric peat layer (0.4 - 1.0 m thick) resting on continuous, ice rich (~50%) permafrost.....	20
Figure 3.6: Varying levels of hydraulic conductivities for 3 types of peat.....	22
Figure 3.7: Decrease in hydraulic conductivity with depth of 3 peatland types.....	23
Figure 3.8: Processes associated to thaw lake expansion and possible catastrophic drainage events.....	25
Figure 4.1: Tertiary and Cretaceous geology underlying Quaternary sediments.....	27
Figure 4.2: Structure of the Yukon Coastal Plain and Barn Mountains.....	29
Figure 4.3: Mean monthly temperatures from 1957-2004.....	35

Figure 4.4: Average Rainfall and snowfall compared to total precipitation.....	36
Figure 4.5: Annual average snow depth versus snowfall on the Yukon Coastal Plain.....	36
Figure 4.6: Ranging values of snow depth from 1957-2004.....	37
Figure 4.7: Change in snow cover extent.....	37
Figure 4.8: Locations of 3 temperate drainage network study sites.....	38
Figure 5.1: Yukon coastal plain digital elevation model (DEM).....	40
Figure 5.2: RiverTools output of all tributaries of the Running River with a pruning threshold of order 3.....	42
Figure 5.3: 1985 Air photograph of the Yukon coastal plain.....	44
Figure 6.1: R_B , R_A , R_L , and R_G of the entire Running River (both open water channels and water tracks).....	45
Figure 6.2: R_B , R_L , R_A , and R_G of identified water tracks.....	47
Figure 6.3: R_B , R_L , R_A , and R_G of open water channels within the Running River (YT).....	48
Figure 6.4: Running River channel profiles of an open water channel (A) and a water track (B).....	51
Figure 6.5: Open water channel profile from the East River, NS.....	53
Figure 6.6: Evolution of Temperate and Arctic networks.....	55
Figure 7.1: A common willow tree as an analogy of the possible branching geometry of Arctic drainage networks.....	58
Figure 7.2: An oak tree as an analogue for the symmetrical, space filling (fractal) nature of temperate drainage networks.....	58
Figure 7.3: Evolution, due to climate change, of a water tracks changing channel profile (Blue) into open water smooth, equilibrium-like longitudinal profile (Red).....	59

List of Tables

	Page
Table 4.1: Attributes of Temperate study Sites.....	39
Table 6.1: Comparative Results Arctic Network Ratios to Temperate Study Ratios.....	49

List of Variables

- A_ω Mean total area contributing of stream order ω
- $D_{\Sigma L}$ Fractal dimension of stream networks using the logs of both the bifurcation R^B and the length R^L ratios
- L_ω Mean length of specified stream order ω
- N_ω Stream segments of any given order ω
- R_A Area ratio: Expression of mean total area contributing to any stream order A_ω compared to the mean total area of the preceding stream order $A_{\omega-1}$
- R_B Bifurcation ratio: Expression of the number of stream segments of any given order N^ω to the number of segments of the next highest order $N_{\omega+1}$
- R_G Gradient Ratio: Expression of the gradient (slope) of stream order ω compared to the gradient of the next preceding stream order $\omega+1$
- R_L Length ratio: Expression of the arithmetic average of the length of a specified stream order L^ω to the average length of two stream orders combining to form the next higher order $L_{\omega+1}$

Acknowledgments

First and foremost I would like to thank Lawrence for all his help on this project. He was always accessible to ask questions and his endless patience, no matter what, was amazing. Working in the lab was like no other work environment I have encountered, and it never seemed like work. To my mom and dad for supporting me on all fronts through four years of university; to my partner in crime Dave for his help with my research and always swearing at the computers louder than me; to Jenn for always making time to help; and to Victoria for always supporting over long distances and always mentioning my name in your theater biographies in all of her shows. Finally to the shores of Nova Scotia for giving endless days of perfect surf, and the citizens of Nova Scotia for teaching me the true meaning of “Easy-going” for these last 4 years.

Chapter 1.0.0: Introduction

1.1.0: Statement of the Problem

For numerous reasons, such as a very short summer and lack of significant human populations, Arctic drainage networks remain a poorly examined facet of fluvial geomorphology. Compared to drainage networks in lower latitudes, Arctic drainage networks occur in different substrates and are shaped by different processes, and may therefore exhibit different properties. Surface and ground water hydrology differ dramatically from non-permafrost areas, because permafrost is an aquiclude that forces water to move as surface flow or through shallow (<1m thick) active layers (French 1996). Low order streams, found at the origin of low latitude drainage networks, may be replaced by small drainage pathways called hillslope water tracks in Arctic networks with continuous tundra land cover (McNamara *et al.* 1998). Water tracks are 1-15 meter wide traceable linear zones of enhanced soil moisture in poorly defined, peat-filled depressions overlying permafrost (McNamara *et al.* 1998).

Thaw lake processes dominate many lowland periglacial environments and, because of this, these regions are classified as thermokarst terrain (French 1996). This terrain consists of full, partly full, and drained thaw lake basins. Lakes drain rapidly on intersecting a drainage pathway such as a river channel (French 1996). The likelihood that these thaw lake drainage events are responsible for the scarce number of incised open water tracks is an additional question posed by this study. In this study, I investigate the following questions: 1) Do drainage networks in the Arctic, where permafrost is continuous, have the same properties as drainage networks in low latitude areas? 2) Are Arctic networks scale invariant, i.e. fractal? 3) What are

the quantitative expressions of the influence of peat and permafrost? 4) How are thaw lake flood events integrated into Arctic fluvial networks?

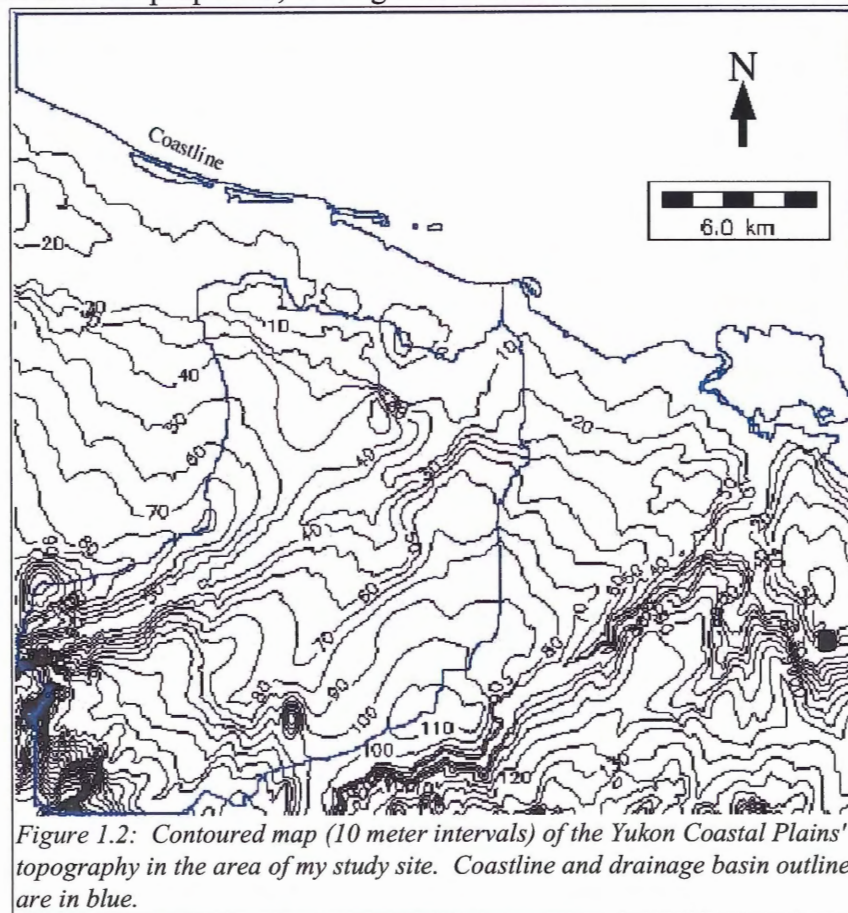
1.2.0: Study Area

The Yukon Coastal Plain is located in the Yukon Territories of northern Canada. This region borders the Beaufort Sea and is laterally bounded by the Mackenzie River to the east, and the Alaska-Canada International border to the west (**Fig. 1.1**).



Lowlands of the Western Canadian Arctic are characterized by low gradient tundra topography (**Fig. 1.2**) of constant tundra composed of a peat layer overlying continuous permafrost. Vegetation is low-lying arctic tundra shrubs and sedges. The combination of peat, permafrost and arid conditions differentiate the Yukon Coastal Plain from temperate regions. The environment is classified as periglacial (French 1996), and dominant geomorphological processes include river systems and thaw lakes. To compare to Yukon Coastal Plain networks, I use temperate networks from the Keg River of northern Alberta, the East River of northeastern

coastal Nova Scotia, and Nicklen Creek of south-central British Columbia. I also use published measurements of network properties, at the global scale.



1.3.0: Previous Work

Numerous papers have used Horton-Strahler models of channel network organization to characterize low latitude networks. My study is unique in that I investigate quantitative properties of high latitude drainage networks, and compare these to existing measurements for temperate networks. However, the properties of Arctic channel networks have been poorly investigated. McNamara *et al.* (1998) examined a small drainage basin (2.2 km²) in northern Alaska to determine whether modern water tracks were related to low order channels that formed

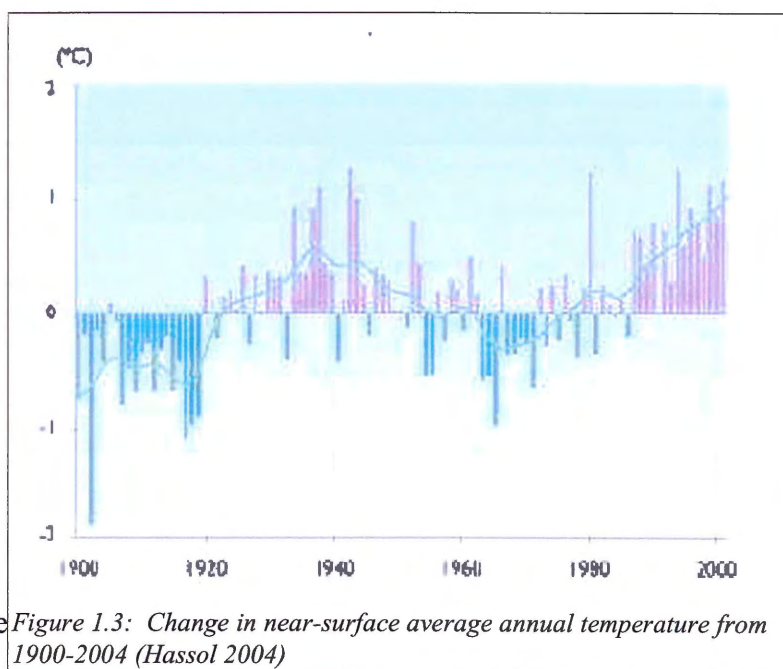
under a warmer, non-permafrost climate, and concluded they were not. Qualities of the water tracks themselves have yet to be quantitatively determined, nor have they been compared to modern analogues of lower latitude drainage networks. The effects of major discharge events, such as thaw lake floods, on the water tracks and larger channels have not been addressed.

1.4.0: Significance

Analysis of their Horton properties may reveal where these water tracks fit into flow paths and the role they play in fluvial transport into the surrounding major river systems (i.e. the Running River). Due to the colder

history of the earth associated to the

last glacial maximum, periglacial conditions possibly similar to current conditions on the Yukon Coastal plain were widespread south of the Laurentide ice sheet. Therefore this study may provide a glimpse of how drainage networks in lowland permafrost evolved into current low stream order systems as observed in low latitudes. Current global warming is affecting Arctic regions, and the Western Canadian Arctic in particular, with annual average temperature increase twice the rate of other locations on earth (Hassol 2004). Over the past few decades, near-surface December-February temperature has increased in northwestern Canada by approximately 3°C (Hassol 2004). Arctic precipitation has increased 8% on average over the past century with



associated increases in river discharge (Hassol 2004). The combination of such factors has led to the thawing of permafrost, lowering of the permafrost table, and 2 ° C temperature increase in permafrost temperatures (Hassol 2004). Melting of permafrost may permit water tracks to evolve by incision into low-order open-water stream presently common at low latitudes. The implications of the drainage network maturation may alter and shape current predictive models as to the evolution of the Canadian Arctic landscape and its major receiving basins.

Chapter 2.0.0: Network Classification and River Morphology

2.1.0: General Background

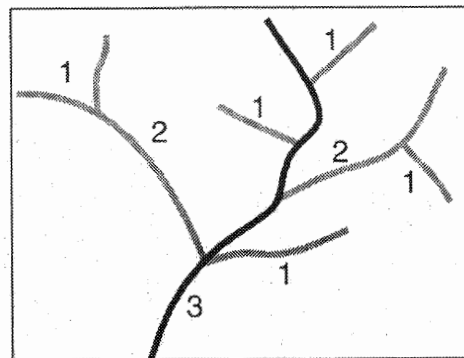
In 1945 R.E. Horton published a quantitative, hydrological approach to the development of streams and their drainage basins. Horton extended Playfair's law in his *Laws of Stream Ordering and Stream Lengths* in order to establish a quantitative meaning (Horton 1945).

Playfair's qualitative law states: "Every river appears to consist of a main trunk, fed from a variety of branches, each running in a valley proportioned to its size, and all of them together forming a system of valleys, communicating with one another, and having such a nice adjustment of their declivities that none of them join

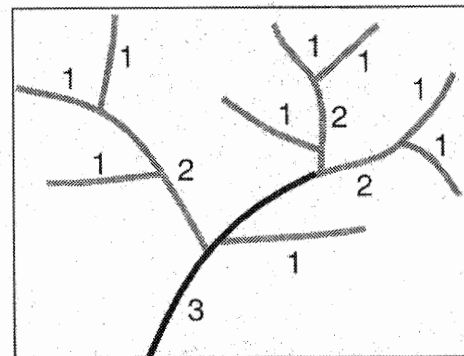
the principal valley either on too high or too low a level." (Tarr and Martin 1914). In 1952, A.N Strahler built on this platform to establish an updated stream ordering scheme that provided a general, spatial

evaluation of common river behavior. This scheme labels source streams order one. When two first order streams join, they become a second order stream, and when two streams of equal order merge, a stream of higher order is formed. When low and high order streams join, the continuing stream retains the order of the higher order stream. **Figure 2.1** shows an

example of Horton-Strahler ordering and link magnitude (Horton 1945). Within a drainage



Horton (1945)



Strahler (1952)

Figure 2.1: River Networks illustrating Horton-Strahler stream ordering (Ritter 2002)

system from source to depocenter, orders become higher, and the physical dimensions of the stream increase, but the total number of stream sequences becomes progressively smaller (Scott 1989).

2.2.0: Fractal Classification

Nature commonly organizes its many systems (including most river networks) in scale independent forms called fractals. A fractal object is one that has self-similar or self affine properties across scales (Mandelbrot 1985). Self-similar means parts of an object are identical to the whole when inspected on either the large or small scale (Mandelbrot 1985). Self-affine means that parts of an object resemble versions of the whole on different scales (Mandelbrot 1985). In reference to drainage networks, similar patterns are seen world wide in numerous geologic settings.

Examples of self-similar fractal organization can be seen in a forest fern (Fig. 2.2) where the small and large scales are identical, and also in self-affine branching river system (Fig. 2.3).

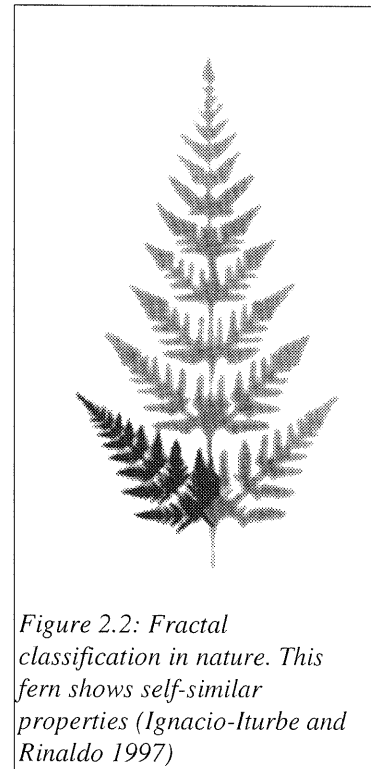


Figure 2.2: Fractal classification in nature. This fern shows self-similar properties (Ignacio-Iturbe and Rinaldo 1997)

2.3.0: Network Properties

R.E Horton developed quantitative expressions to characterize basin properties now called “Horton Laws”, which were subsequently adopted and extended by Strahler and others. Determination of network specific ratios is the first step as these values are then analyzed against each other to establish unique drainage attributes. The two fundamental laws, which

describe the numbers and lengths of streams of different orders in a drainage basin are: 1) The law of stream numbers (R_B), and, 2) The Law of stream lengths (R_L) (Horton 1945). Subsequent Hortonian laws deal with specific stream characteristics that are useful in basin comparisons.

Horton's Law of Stream Ordering

Drainage networks commonly display a patterning that is independent of scale. Horton's law of stream ordering represents these formal relations between parts of the drainage network numerically. This equation shows the relationship between the number of streams of a given order and the stream order in terms of an inverse geometric series, to which the bifurcation ratio is the base (Horton 1945).

Bifurcation ratio (R_B) is a ratio between the number of stream segments of any given order (N_ω) to the number of segments of the next highest order ($N_{\omega+1}$) according to:

$$R_B = \frac{N_\omega}{N_{\omega+1}} \tag{1}$$

A R_B of 3.0 for stream order one denotes that there is three times as many first order streams as second order. Bifurcation ratio ranges are 3-5, with ~4 most common (Rodriguez-Iturbe and Rinaldo 1997).

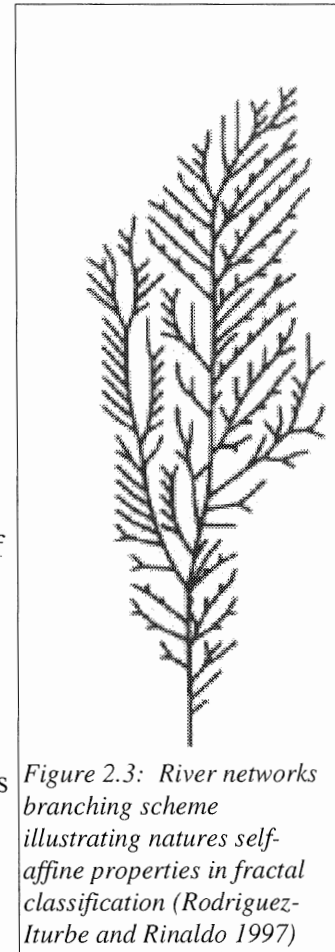


Figure 2.3: River networks branching scheme illustrating nature's self-affine properties in fractal classification (Rodriguez-Iturbe and Rinaldo 1997)

Horton Law of Stream lengths

The length ratio (R_L) describes how a stream/river length increases with order (i.e. segments get longer as order increases). This ratio is a comparison of the arithmetic average of the length of a specified stream order (L_ω) to the average length of the next order ($L_{\omega+1}$) stream according to:

$$R_L = \frac{\bar{L}_\omega}{\bar{L}_{\omega+1}} \quad (2)$$

Length ratios range from 1.5-3.5 with values of 2 most common, but are dependent on the drainage network itself and specified order (Rodriguez-Iturbe and Rinaldo 1997).

Schumm's Law of Stream Areas

Horton did not include basin areas in his defined laws of drainage basin composition. He however, did imply that areas should satisfy a geometric series as he stated for stream numbers and lengths. Schumm took Horton's basis and explicitly stated his law of stream areas. The law is expressed as:

$$R_A = \frac{\bar{A}_\omega}{\bar{A}_{\omega+1}} \quad (3)$$

The area ratio (R_A) is an expression of the mean total area contributing to any stream order (A_ω) compared to the mean total area of the preceding stream order ($A_{\omega-1}$). Like previous geometric series, of length and numbers, basin areas will abide to similar behavior. The largest order to form in a network is directly related to the spatial attributes and size of the basin it is contained in. A mean ratio of 5 across all orders is common.

Gradient Ratio

The gradient ratio (R_G) is an expression of the mean slope gradient of a stream order (G_ω) compared to the mean slope gradient of the next order ($G_{\omega+1}$). R_G is expressed as:

$$R_G = \frac{\bar{G}_\omega}{\bar{G}_{\omega+1}} \quad (4)$$

Fractal Dimension of Stream Networks

Tarboton (1988) derived a numeric relation between fractal dimension of stream networks using the logs of both the bifurcation (R_B) and the length (R_L) ratios. Utilizing the logs of these ratios, the possibility of classifying a stream under fractal classification is expressed as :

$$D_{\Sigma L} = \frac{\log(R_B)}{\log(R_L)} \quad (5)$$

Numerous authors have interpreted the value of $D_{\Sigma L}$ as a possible measure indicating the degree of randomness of the stream network evolution (Cheng *et al.* 2000). Common values of $D_{\Sigma L}$ are close to 2, denoting that stream networks in the entire area with this value, statistically satisfy a space filling property (Cheng *et al.* 2000).

In this case, fractal classification is achieved. Stream networks, if any, above/below the value of 2 are likely not fractals.

2.4.0: Graphical Representation of Hortons Laws for Measured Networks

Horton numbers, R_B , R_A , R_L , for a drainage basin are commonly viewed using semi-log plots of mean channel length, bifurcation, and area versus stream order. **Figure 2.4** illustrates Hortonian laws for the Mamon River basin in Venezuela (Rodriguez-Iturbe and Rinaldo 1997).

Plots utilized in this study are; along-channel length versus drainage area, Strahler order versus along-channel length, Strahler order versus drainage density, drainage area versus along-channel slope, Strahler order versus along-channel slope, and Strahler order versus drainage area. These relationships plot as straight lines in semi-log plots (Fig. 2.4).

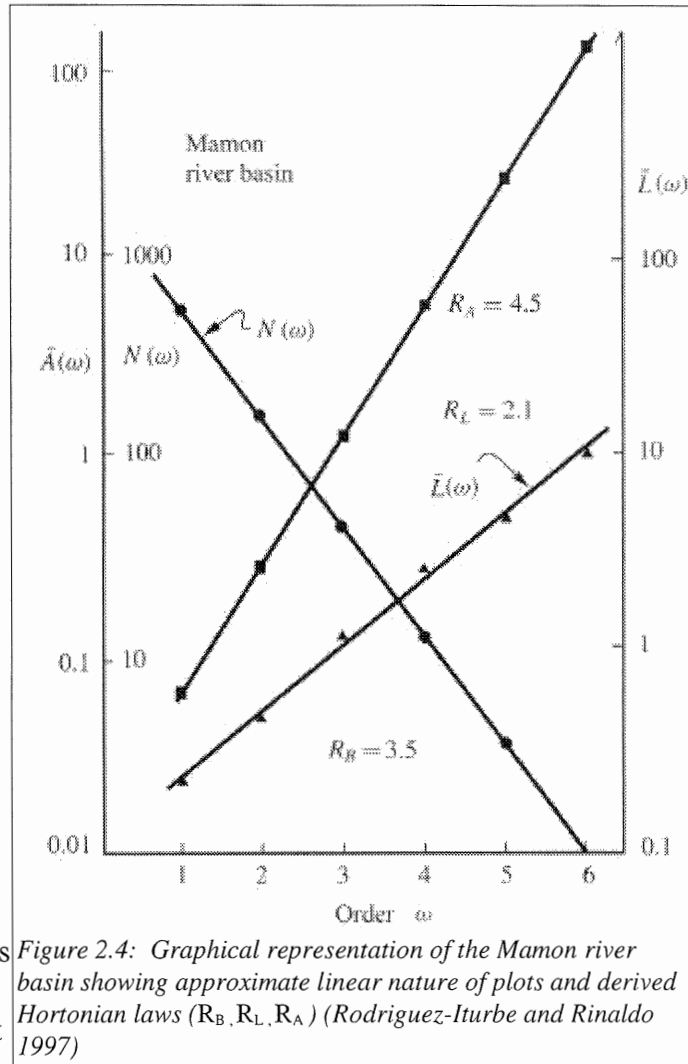
2.4.1: Strahler Order versus Stream Numbers

Plotting stream numbers of a specific basin against Strahler orders, a negative sloped, linear plot is formed (Fig. 2.4). The slope of this line is Horton's law of stream numbers (R_B -bifurcation ratio).

2.4.2: Stream Ratios

Plotting along-channel length versus Strahler order, a positive sloped, linear plot is formed (Fig. 2.4). By determining the slope of this line, Horton's law of stream length (R_L) is derived. The cumulative nature of Horton's stream ordering scheme is shown as one increases order, the overall length of streams is also increasing.

Plotting drainage area of a specified basin versus Strahler order, a positive slope, linear plot is formed (Fig. 2.4). The slope of this line corresponds to Horton/Schumms' Law of Stream



Areas (R_A). The positive slope intuitively depicts as one increases stream order, the basin areas that these larger streams drain increases.

2.5.0: Hortonian Qualitative Erosional Evolution of Streams

Horton's description of the erosion development of streams compliments his quantitative formulas. A large fundamental aspect is his infiltration theory of surface runoff (Horton 1945). The importance of this theory is directly related to the amount of precipitation allowed to encroach a surface in order to entrain and transport exposed sediments. This defines the initiation of an eroded drainage network. The theory is based on two fundamental concepts (Horton 1945):

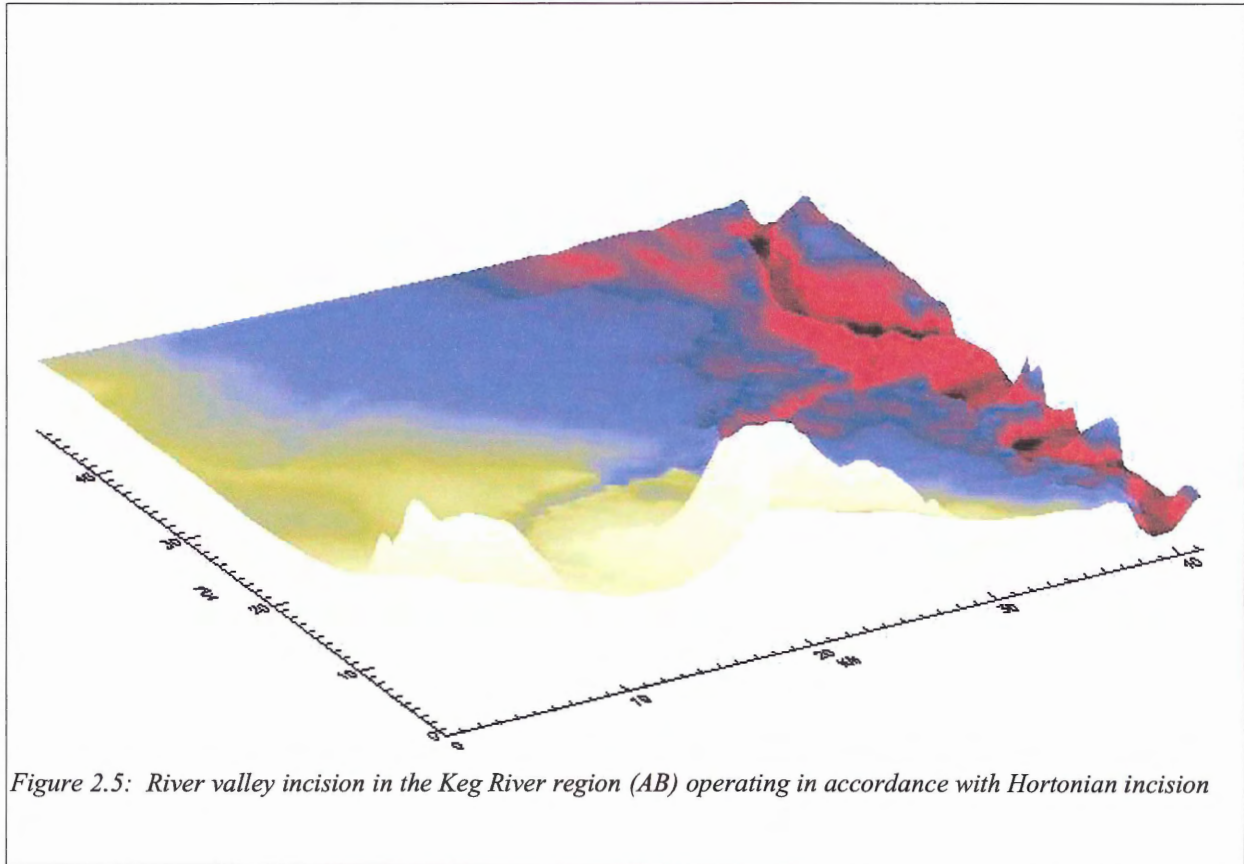
- (1) There is a maximum or limiting rate at which the soil, when in a given condition, can absorb precipitation as it falls and is labeled the infiltration-capacity.
- (2) When runoff takes place from any soil surface, there is a definite functional relation between the depth of the surface detention, or the quantity of water accumulated on the soil surface, and the rate of surface runoff or channel inflow.

For a specified terrain there would be a minimum length of overland flow required to produce sufficient runoff volume to initiate erosion (Horton 1945). Within this length, simple hydraulic transportation is occurring with inappreciable sheet-like erosion. This length varies from network to network, depending on surface slope, runoff intensity (rate in m/hour), infiltration-capacity, and resistivity of the soil to erosion (a proportional factor representing the quality of material which can be entrained) (Horton 1945). If the quantity of material entrained and carried

in overland flow exceeds the quantity which can be transported, deposition or sedimentation on the soil surface will take the place of erosion (Strahler 1952).

According to Horton's conceptual model for network development, channel initiation occurs on newly exposed terrain that lacks regeneration of sorts (i.e. deposition). The cycle begins with sheet erosion spreading laterally as the minimum length (critical distance) is exceeded as the width of the exposed terrain increases (Horton 1945). Minor, shallow, closely-spaced, parallel, "shoestring" rills develop in this early phase (Horton 1945). Diversion of flow from shallow to deeper rills progresses and results in a cross-grading (Horton 1945). With newly exposed terrains, streams starting at these points become primary, or highest order streams of the ultimate drainage basin (Horton 1945). Rilled surfaces develop on either side of the main stream, followed by the cross grading process. Rills mature and connect to form channels. Eventually the length of overland flow in remaining areas will be less than the critical length (Horton 1945). This process accounts for the geometric series, defined by Horton's equations (i.e. stream numbers and lengths), observed in drainage basins. As more and more terrain is eroded and exposed, weaker streams are absorbed by the stronger, larger streams by competitive erosion, and the drainage basin grows in width along with its length (**Fig. 2.5**) (Horton 1945). These two do not occur at the same rates resulting the common pear shaped basin. Erosion and sediment supply limit the size of the basin. Belts of no erosion separate incised channels for periods of time until the point, via conditions such as flooding, erosion overwhelms the belt. Stream channels, however, generally do not extend to the watershed line (Horton 1945). Valleys can not grade below the stream level and the valley supplies the run off and sediment which both

determine the valley and stream profiles (Fig. 2.5) (Horton 1945). A complex balance between precipitation, slope, critical length, sediment supply and type, generally determines the final geometry.



2.6.0: Alluvial and Fluvial River Processes

Alluvial stream flow across material previously deposited by the stream itself (Ashmore and Church 2001). Bedrock streams are those constrained by durable or brittle, underlying bedrock beneath the channel bed (Ashmore and Church 2001). Recognition of four channel

styles, observed in global drainage networks, was possible by examining larger scale river features.

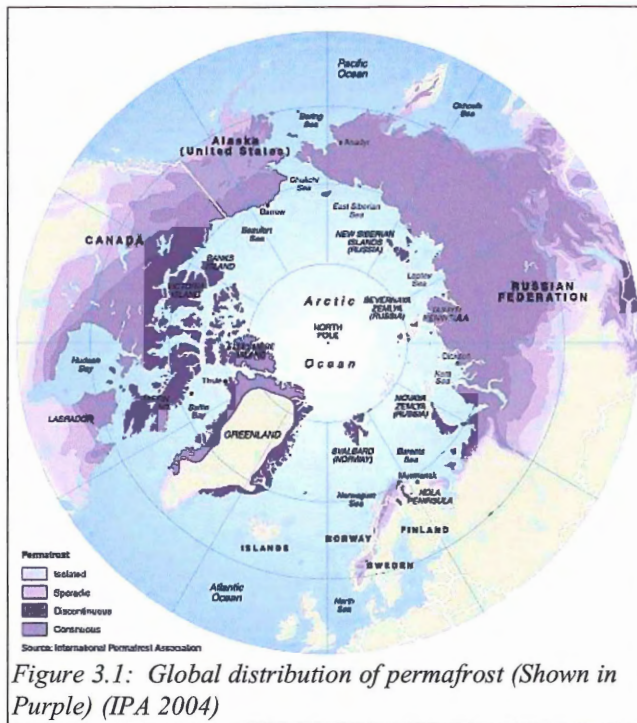
The four channel styles are straight, braided, meandering, and anastomosing (Miall 1992). The mechanics of transportation within these channels also requires classification into two primary mechanisms. The first is via traction currents that transports cohesion less sediment as individual grains (Miall 1992). The second through sediment gravity flows by mass transport of sediment by liquefaction on sloping surfaces (Miall 1992). In this process large grains slide and roll along river beds as bedload and smaller grains bounce down the river bed as they are held in suspension for short periods of time as bed contact load (Miall 1992). In either case, quantity of grains in Arctic drainage networks is very small. The competency and capacity of the river/stream itself defines the its' ability to transport material. Competency refers to the strength of flow in a river through velocity and shear stress, and is an indication as to the maximum grain size a river can transport (Miall 1992). Capacity is the total volume of sediment that can be moved (Miall 1992). Competency and capacity both depend on river discharge. High latitude drainage networks have little to no flow in low to medium order channels in winter. Because water flows for only a short period of the year, its effects in shaping the periglacial landscape are minimal (Ashmore and Church 2001).

Chapter 3.0.0: Arctic Peat, Permafrost and Rivers

3.1.0: General Background

The Yukon Coastal Plain is a region characterized by flat topography, continuous permafrost and peat accumulation. These, combined with the associated cold Arctic temperatures and low annual precipitation (Section 4.5.0) drain Arctic watersheds. Examining properties of peat and permafrost is therefore a very useful approach to an overall understanding of the processes driving Arctic drainage networks.

3.2.0: Permafrost Categorization



The term permafrost refers to a combination of soil and rock that remains below 0°C for two years or longer (French 1996). Contrary to intuition, permafrost does not necessarily form at all locations where the ground surface temperature is less than 0°C . Temperatures significantly below 0°C are often required to initiate the change of pore water into ice (Anderson and Morgenstern 1973). The occurrence and magnitude of the

depression in the initial freezing point depends on factors such as fluid pressure, salt content of the pore water, the grain size distribution, the soil mineralogy, and the soil structure (van Everdingen 1976). After the initial freezing point has been reached, a sharp drop off of liquid

water content occurs when the temperature is less than 0° C (van Everdingen 1976). Frozen ground in the Yukon coastal plain is ice rich (~50%) (Williams and Smith 1989). This is accomplished as permafrost exists at depths where seasonal temperature variations are insufficient to thaw the ground (Williams and Smith 1989). Extended cold periods in winter combined with relatively short warm summer periods, allow continued presence of permafrost.

Permafrost formation is believed to have originated during the Pleistocene epoch, but variances likely occurred depending on regional conditions (Linell and Tedrow 1981). Permafrost globally occurs in four distinctive

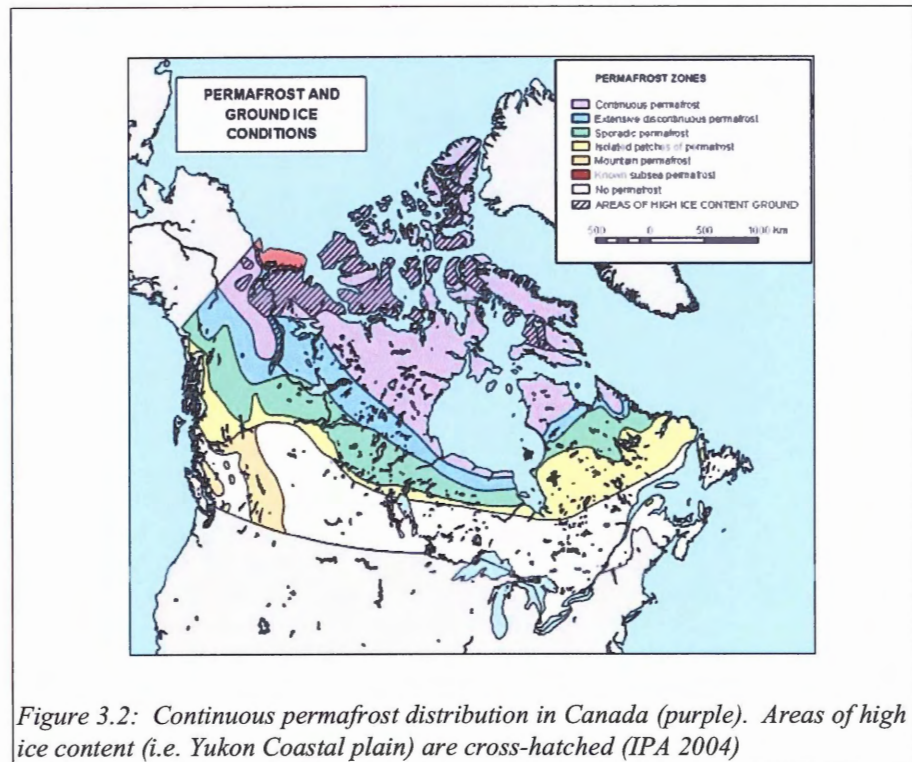


Figure 3.2: Continuous permafrost distribution in Canada (purple). Areas of high ice content (i.e. Yukon Coastal plain) are cross-hatched (IPA 2004)

environments; the Alpine, high latitude, plateau, and sub-sea environments (French 1996).

Typically as one moves to lower latitudes, annual mean temperatures generally increase allowing increased thawing of cryotic ground, or prevention of the accumulation/formation of permafrost.

French (1996) determined the limiting mean annual air temperature for continuous permafrost zones to be -6 - -8° C . Continuous permafrost in Arctic Canada is measured to be up to 400 meters thick (Linell and Tedrow 1981). Specific reference to permafrost in this paper involves

high latitude, continuous permafrost (**Fig. 3.2**). An active layer exists above the defined permafrost table. This is a layer that freezes and thaws seasonally (French 1996). Thickness and composition of this layer varies widely depending on ambient air temperature, vegetation, drainage, soil and rock type, water content, snow cover, slope, and orientation (French 1996).

Permafrost has three temperature defined states; frozen (cryotic), partially frozen, and non cryotic (unfrozen for indefinite length of time annually) (Williams and Smith, 1989). These unfrozen sections, or layers, are labeled taliks in some literature (**Fig. 3.3**).

These features can be contained within the permafrost (intra-permafrost) or sub-permafrost

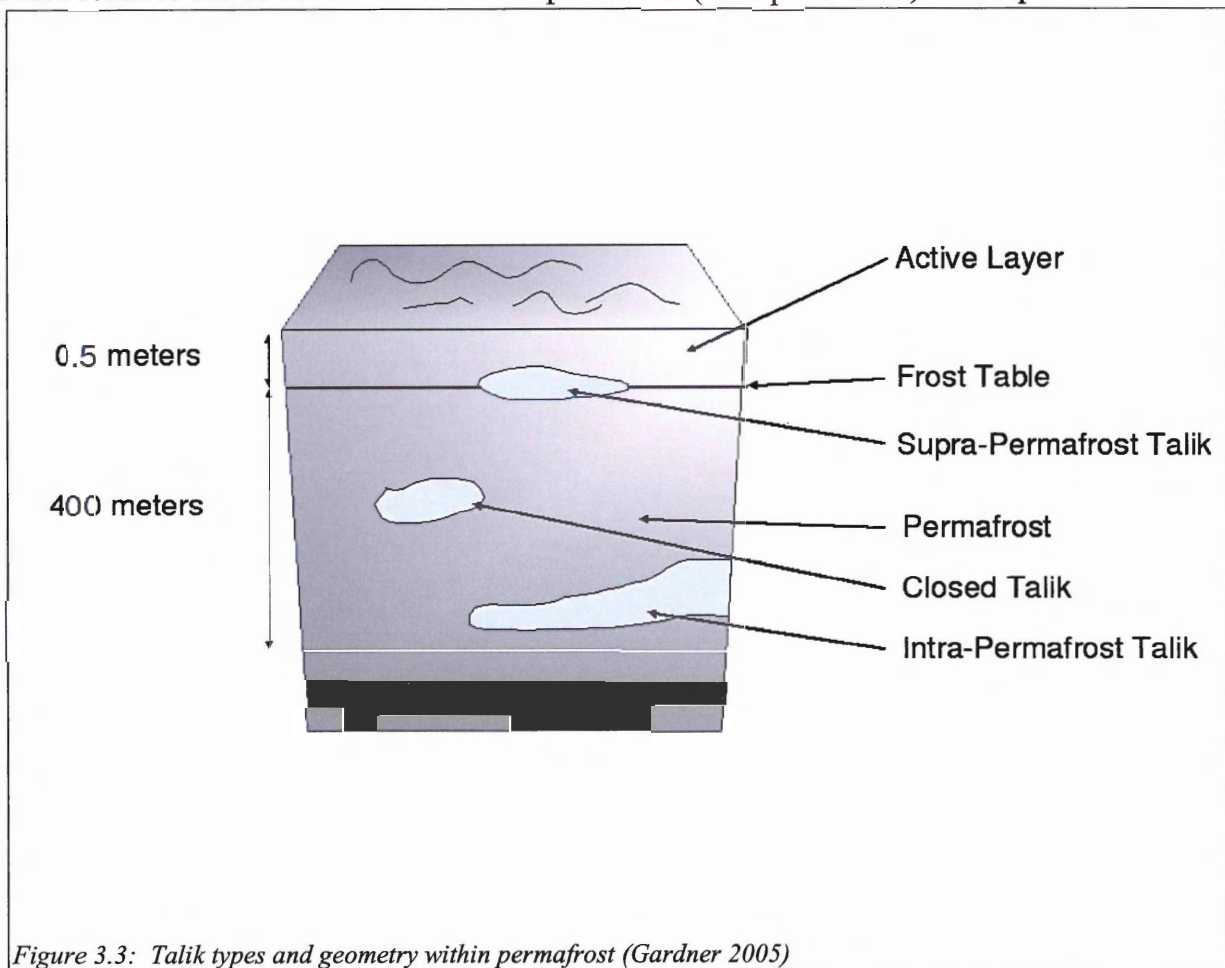


Figure 3.3: Talik types and geometry within permafrost (Gardner 2005)

Taliks, being below the layer (**Fig. 3.3**). Warm summers, water infiltration, or topographic

inequalities are likely causes of these generally temporary, thawed out features. Mineral content also plays an important role as mineralization of ground water can lower the waters freezing point. Features, such as ice wedge polygons and frost heaves speckle the Arctic landscape as water freezes. At 0° C, pure water will freeze and expand by approximately 9% of its original unfrozen volume (Williams and Smith 1989). Water/ice is the only substance on earth to expand upon freezing, and judging by the vast amount of ice laden permafrost, may provide unique results on drainage through such a substrate.

3.2.1: Hydraulic Properties of Permafrost

The hydrological importance of permafrost rests in the large differences in hydraulic conductivity that have been determined for most geologic materials between their frozen and unfrozen states (Williams and Smith 1989). **Figure 3.4** shows the changes in hydraulic conductivity of geologic materials as temperature decreases. The content of unfrozen water decreases and the pore ice content increases as temperature is lowered from 0°C toward -1°C . Hydraulic conductivity declines by several orders of magnitude as

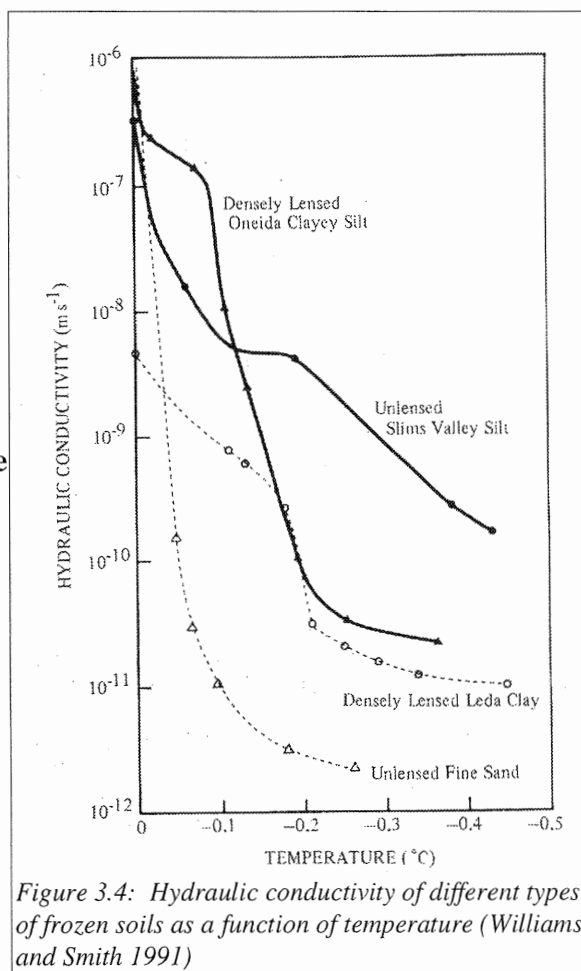


Figure 3.4: Hydraulic conductivity of different types of frozen soils as a function of temperature (Williams and Smith 1991)

temperature falls a small amount below 0° C (**Fig. 3.4**). A sand substrate is also depicted in **Figure 3.4** and sand typically could be an aquifer in unfrozen states in appropriate stratigraphic

conditions. Slightly below 0°C the sand becomes a low permeability aquitard. This exemplifies the effects freezing has on a material.

Perennially and seasonally frozen ground prevents the infiltration of water into ground, or at best, confines it to the

active layer (French 1996).

This results in a high percentage of surface runoff and minimal recharge of groundwater systems, if any.

Moisture within permafrost itself migrates in response to a temperature gradient in upper few meters of permafrost (French 1996).

Groundwater movement in permafrost is restricted by the presence of both perennially and seasonally frozen ground because the ice acts as a

confining layer of surface and subsurface water (French 1996). This impermeability, combined

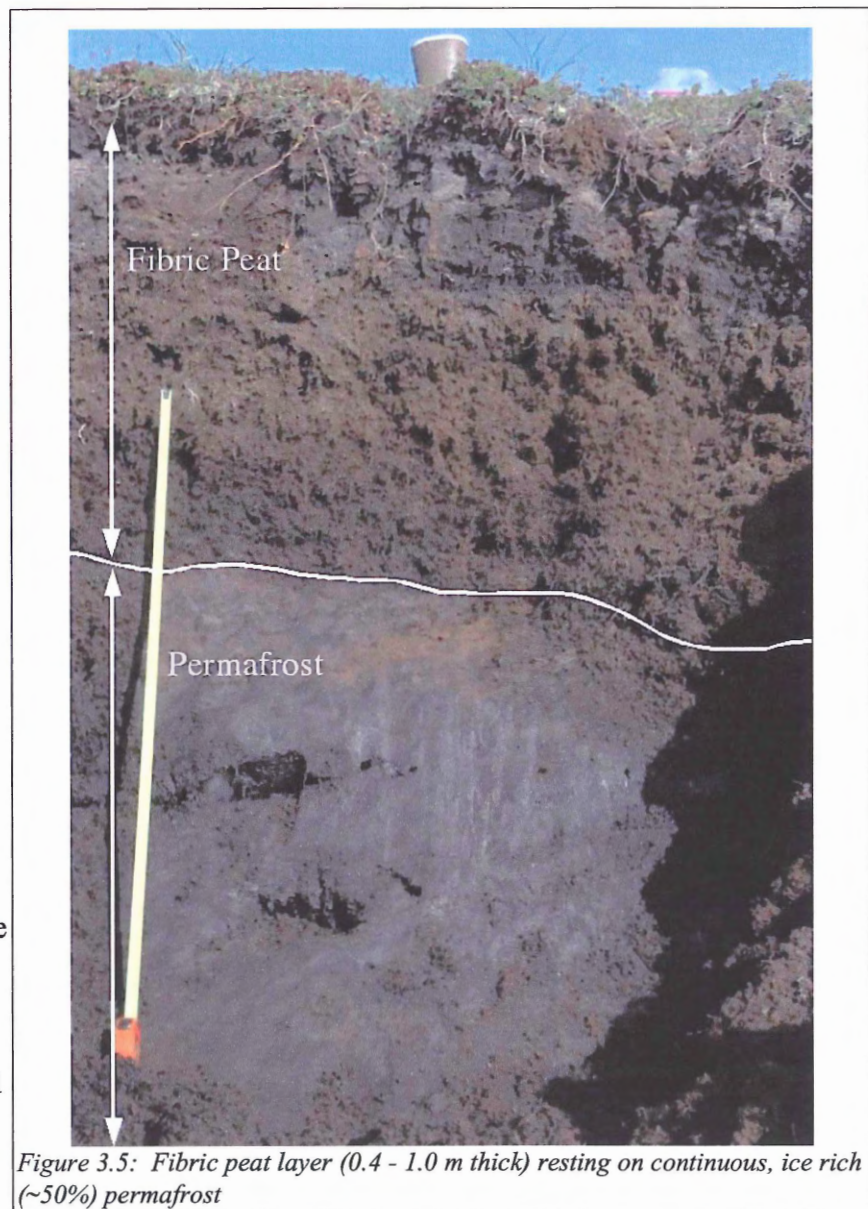


Figure 3.5: Fibric peat layer (0.4 - 1.0 m thick) resting on continuous, ice rich (~50%) permafrost

with porous overlying peat layers, restricts subsurface flow to unfrozen zones or taliks (**Fig. 3.3**) (French 1996).

3.3.0: Peat

Peat is the primary organic matter of the Yukon Coastal Plain. Due to the cold nature of the Arctic, dead organic matter does not readily decompose (Boelter 1969). As a result, the Yukon coastal plain is a continuous “mat” of peat resting on continuous permafrost (**Fig. 3.5**). It is in this setting that surface water is transported from the watershed.

3.3.1: Peat As An Insulator

Peat shields permafrost from solar heat and melting. Removal or even disruption of the overlying cover causes melting of the underlying permafrost (**Fig. 3.4**). In continuous zones this could result in the lowering of the permafrost table. Thermal conductivity of the peat varies through the year. During the summer the surface layers of peat become dry through evaporation. The thermal conductivity of peat is low during this time and warming of the underlying soil is impeded (Brown 1966). When peat freezes the thermal conductivity of peat increases considerably (Brown 1966). Peat therefore offers less resistance to the cooling of the underlying soil in the winter than to the warming in the summer contributing to permafrost being frozen, and therefore impermeable, year round. The thermal conductivity of saturated frozen, saturated unfrozen, and dry peat is 2.00, 0.50, and 0.05 W/m K respectively (French 1996).

3.3.2: Hydraulic Properties of Peat

Peat is a very porous medium with a very high hydraulic conductivity (**Fig. 3.6**). The combination of the underlying impermeable permafrost and this porous fabric, no overland flow is permitted above the peat layer (**Fig. 3.3**). The rate at which water will move through a peatland is dependent on the pressure of water and the resistance to it (Baird and Heathwaite 1997). Poorly compacted, peat with large plant fragments typically has large pore spaces and therefore a high hydraulic conductivity (Baird and Heathwaite 1997). This is the case for the

Yukon coastal plain. Rycroft *et al.* (1975) suggested a hydraulic conductivity range from 6×10^{-6} - 5×10^{-3} cm s^{-1} from a combination of previously published literature values. Chason and Siegel (1986) expanded this range to 10^{-1} - 10^{-7} cm s^{-1} and 10^{-1} - 10^{-6} cm s^{-1} from field observations and laboratory experiments respectively. Hydraulic conductivity has been shown to vary with depth (**Fig. 3.7**) (Chason and Siegel 1986). Additionally, the potential for horizontal movement at depth may be much greater than vertical movement (Chason and Siegel 1986). Figure 3.6 illustrates this change in

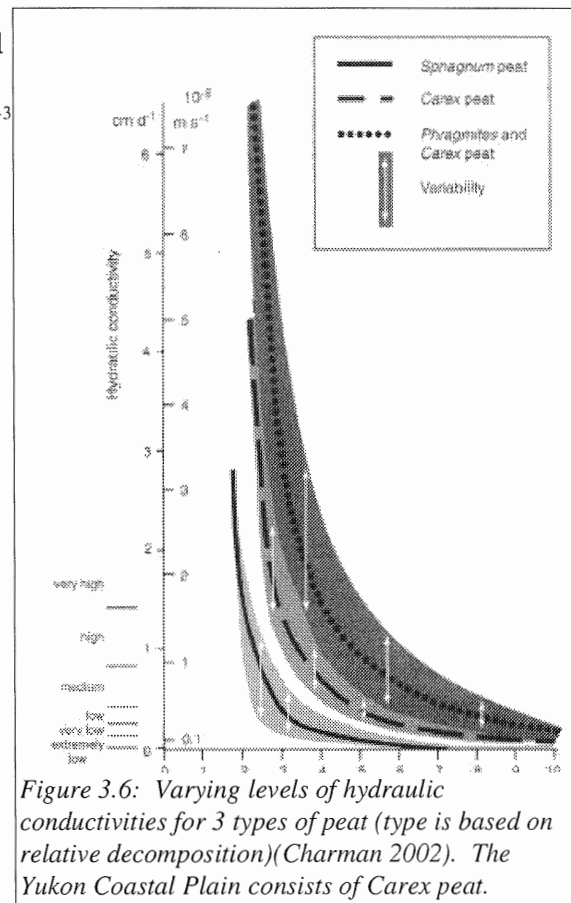


Figure 3.6: Varying levels of hydraulic conductivities for 3 types of peat (type is based on relative decomposition)(Charman 2002). The Yukon Coastal Plain consists of Carex peat.

hydraulic conductivity of three peatland types. **Figure 3.6** also illustrates that the upper layer of the peatland has the highest hydraulic conductivity and will therefore be the most efficient

drainage mechanism. During runoff periods, this area will be crucial in transporting excess water (Baird 1997). Quinton *et al.* (2000) determined the subsurface flow regime within peatlands to be laminar. Leopold *et al.* (1992) documents the difference in erosive power of laminar and turbulent flow regimes. Documentation of overland flow regimes erosive power is also common in hydrology literature (Leopold *et al.* 1992).

3.4.0: Arctic Rivers

Stream flow response to variations in precipitation are rapid, because all subsurface water flow is restricted to the thin active layer above the permafrost table (Williams and Smith 1989). Groundwater contribution to stream flow is therefore negligible in the Yukon coastal plains' continuous permafrost regions (Williams and Smith 1989). Peak discharge in Arctic channels occurs during the spring melt, for a short duration of days to week intervals (Williams and Smith 1989). The Yukon coastal plain receives very little precipitation annually (Section 4.5) and despite low winter temperatures (Fig. 4.3), minimal snow accumulation occurs (Fig. 4.5). Fluvial processes are strongly influenced by the presence of permafrost at depth, and by snow/ice cover in winter months (Woo and Sariol 1981). Classification of river channels on the Yukon coastal plain have coarse, clastic boundaries, and a characteristically high width to depth ratio (McDonald and Lewis 1973). Primary modes of sediment transport are as bedload and channel

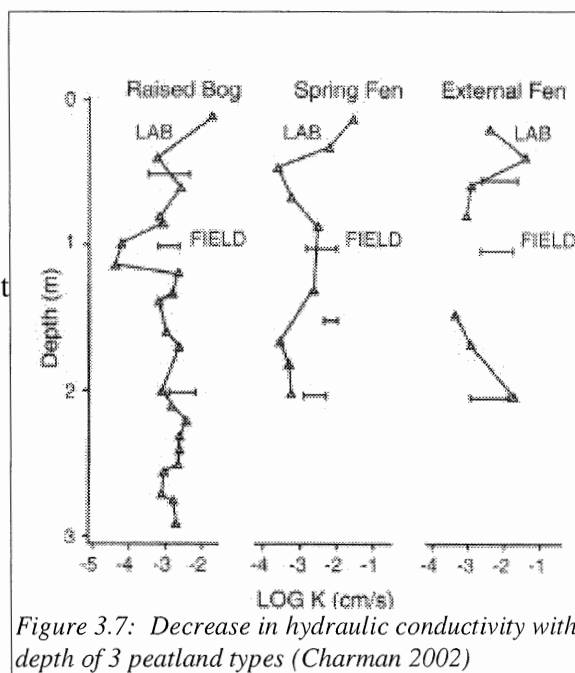


Figure 3.7: Decrease in hydraulic conductivity with depth of 3 peatland types (Charman 2002)

beds are armored by selective transport of sediment grains and imbrication of grains (McDonald and Lewis 1973).

3.5.0: Thaw Lake and Thermokarst Topography

The term thermokarst refers to groups of ground ice related features that form from the melting and collapse of permafrost due to water loss (French 1996). The groups consist of three types of depression like features called Alas, ice wedges, and thaw lakes (Ritter 2002). Thaw lakes are topographic depressions formed as a result of melting of the underlying, ice-rich permafrost (French 1996). The Yukon coastal plain consists of numerous thaw lakes speckling the landscape and due to their relative abundance and associated water volumes, impact the behavior of Arctic drainage networks. Specifically, these lakes release large volumes of water when the gradual warming of the lake water initiates bank collapse and the lake drains in a short amount of time (**Fig. 3.8**) (hours to days) (French 1996).

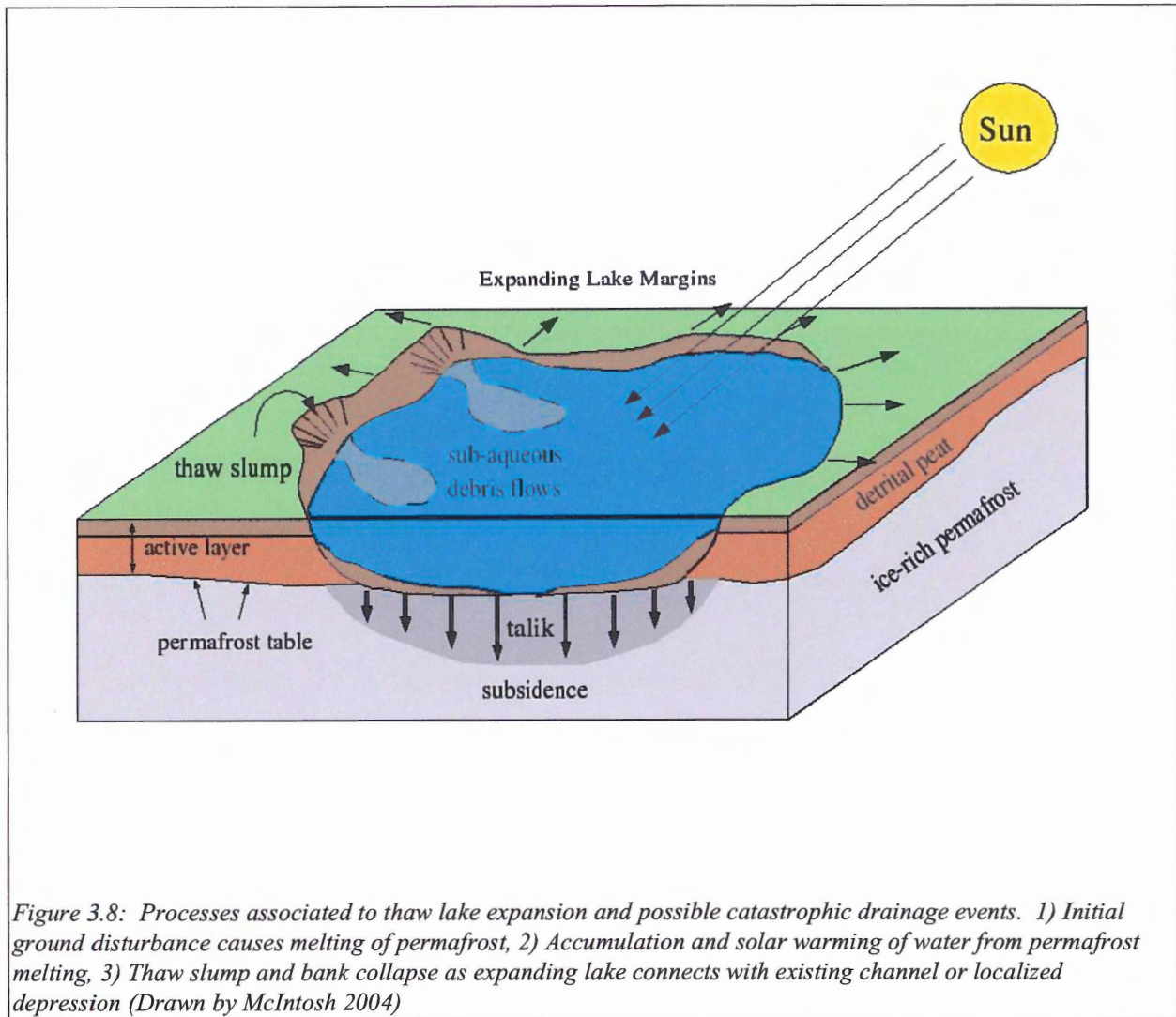


Figure 3.8: Processes associated to thaw lake expansion and possible catastrophic drainage events. 1) Initial ground disturbance causes melting of permafrost, 2) Accumulation and solar warming of water from permafrost melting, 3) Thaw slump and bank collapse as expanding lake connects with existing channel or localized depression (Drawn by McIntosh 2004)

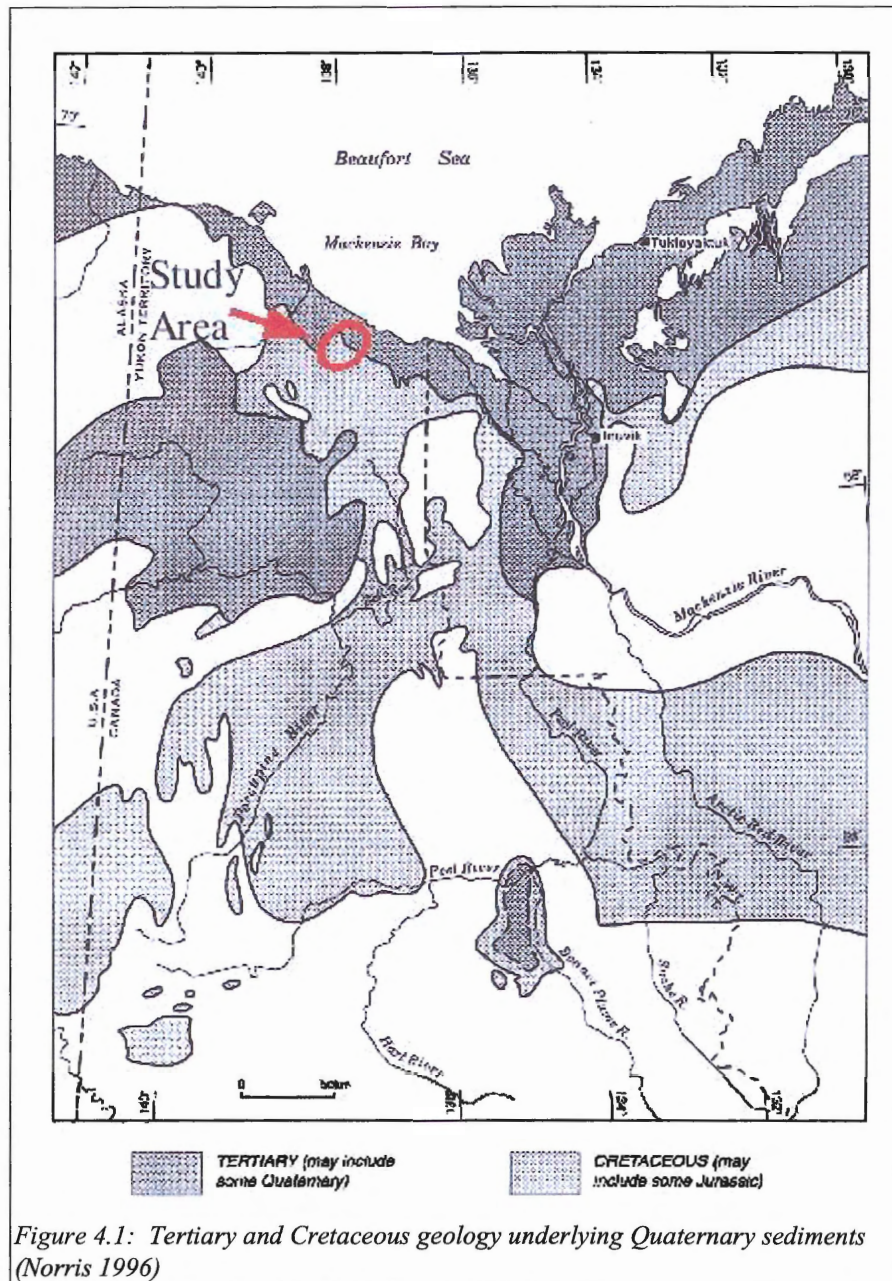
4.0.0: Field Locations

Geologic history of the Tertiary and Quaternary Periods of the Yukon Coastal Plain will be addressed in this chapter. The Barn Mountain river basin source area of the Yukon coastal plain are described (**Fig. 4.1**). Included are recent and past climatic shifts in the area due to their importance in river systems dynamics.

4.1.0: Yukon Coastal Plain

The Yukon Coast Plain includes all flat and gently sloping terrain between the British, Barn, and Richardson Mountains fringing the Beaufort Sea (**Fig. 4.1**) (Rampton 1982). The boundary between the Barn Mountains and coastal plain is regularly delineated by escarpments. The pediment, formed during the late to middle Tertiary, truncates strata of Paleocene age, yet is covered by Pleistocene sediments (Rampton 1982). Erosional and depositional events played a significant role in constructing the Yukon Coastal Plain. The transgression and regression of the Beaufort Sea and Arctic Ocean was the environment in which these mechanisms dominated (Norris 1997). Jurassic and Lower Cretaceous deposition of shales and sandstones formed the onshore sequences of the Beaufort shelf. The Yukon Coastal Plain is a landward extension of the Beaufort Sea (Rampton 1982). Sections of the examined Running River reveal units of Upper Cretaceous conglomerates, sandstones, shales, and mudstones underlain by Tertiary aged conglomerates, sandstones, shales and coal layers (Norris 1996). Structural elements in the area include northeast trending faults and folds beneath the coastal plain and will be discussed further in **Section 4.2.0 (Fig. 4.2)**.

4.2.0: Bedrock Geology



Major uplift events that characterize the topography of the Yukon Coastal plain occurred during the Tertiary. The formation of the river sourcing the Barn Mountains (Fig. 4.2) is an

example of this uplift associated to the Canadian Cordillera (Dyke 1996). The Barn Mountains are a group of low hills and mountains between the Babbage and Blow rivers (**Fig. 4.2**) (Rampton 1982). Elevation does not exceed 1100 m and local relief is commonly 460 m (Rampton 1982). This uplift is generalized as a number of elongate blocks bounded by sub-vertical, north-trending, curvilinear, listric, generally eastward-verging contraction faults active in the Ellesmerian Orogeny (**Fig. 4.2**) (Rampton 1982). The Barn Mountains are the surface manifestation of the Barn Uplift and are bounded between the Old Crow plateau and the dextral Bran fault (Norris 1996). It is situated as the easternmost part of the Romanzof Uplift. Within this structure are imbricated southwest dipping thrust faults and open folds with northwest trending axial tracts (Norris 1996). The Kaltag fault is a major Cretaceous fault resulting from the interaction of drifting continental plates (Norris 1996). The southeastern edge of the Barn Mountains coincides with the western edge of the Rapid Creek Fault array which is a component of the larger Kaltag fault (**Fig. 4.2**) (Norris 1996). Named formations in this area are; the intensely folded Neruokpuk Formation consisting of a lower unit of limestone, shale and a upper unit of argillite and lithic sandstone; the Carboniferous Kekiktuk and Kyak formations composed of chert, conglomerate, quartzite, shale, coal and limestone; the Triassic Shublick Formation composed of limestone; the Jurassic Kingak Formation composed of shale; and Cretaceous shale and sandstone (Norris 1996). Exposed Devonian porphyritic granite in sections is a byproduct of the Ellesmerian Orogeny (**Fig. 4.5**) (Norris 1996). Specifically in the region of the Running River, Upper Cretaceous conglomerates, sandstones, shales, and coal layers are present (Rampton 1982).

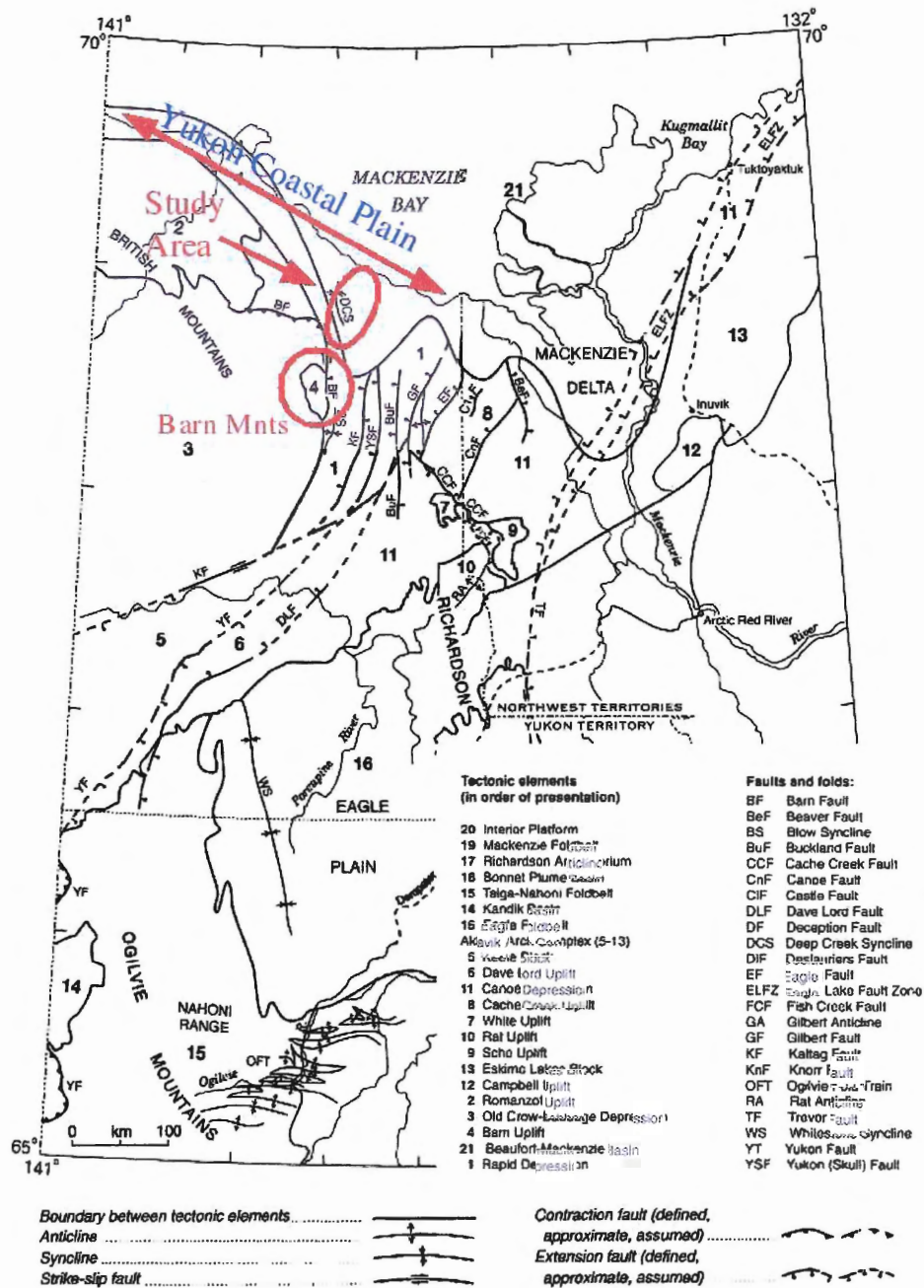


Figure 4.2: Structure of the Yukon Coastal Plain and Barn mountains (Norris 1996)

Sediments predating the uplift are chiefly marine in nature. A dominant rifting phase corresponds to the early Jurassic through to the mid Aptian (Norris 1996) and is associated with the extension in the North America Craton which would eventually lead to the formation of oceanic crust in the Canadian Basin (Norris 1996). East-Southeast derived sediments were deposited on the Cratonic Shelf. During this phase of tectonic activity, fault bounded uplifts and depressions characterized the Northern Yukon (Norris 1996). The Blow Trough is an example of such rapid depression. These grabens then became major sites for deposition as bathymetric and tectonic troughs (Norris 1996). These troughs, labeled the British-Barn troughs, became infilled during the late Aptian/Early Albian as a major transgression occurred (Norris 1996). Tertiary strata are now rendered as deltaic and/or delta front environments (**Fig. 4.1**) (Norris 1996). Previously mentioned rock types such as chert, limestone, argillite, conglomerate, shale, and sandstone are in their embryonic form. These rock types imply a deep basin or basin margin environment.

Tectonic forces changed during the Early Tertiary from a rifting to horizontal compressional forces producing structural relief (**Fig. 4.2**) (Norris 1996). These forces were a component of the north most Canadian Cordillera (Norris 1996). This uplift signaled a hiatus in deposition. Movement from this compression was along a closely spaced series of contraction faults and resulted in thickening of this section (Norris 1996). Uplift was greatest on the east side of the mountains and is supported by steep dips of the Kingak and Kekiktuk formations (Norris 1996). Tertiary sediments have been uplifted to form the topographical relief, prior to erosion, seen today.

4.3.0: Quaternary Geology

Like many locations worldwide, the Quaternary Period of the Yukon coastal plain experienced the effects of dynamic glaciers. My study area on the Yukon Coastal Plain was exempt from the effects of the Last Glacial Maximum due to its location between major ice sheets, and the Western Cordillera (Rampton 1982). The Quaternary geology of the Yukon Coastal plain is divided into three sub-categories: 1) pre-glacial, 2) glacial, and 3) post-glacial. The pre-glacial consists of basinal marine sediments and their associated uplift events outlined in **Section 4.2**. Complex marine, deltaic, fluvial, lacustrine, and terrestrial sediments were deposited and exposed (Rampton 1982). Fluctuating degrees of erosion and deposition occurred in accordance with varying climatic conditions. Large alluvial fans on pediment surfaces and isolated altiplanation terraces in higher elevations formed during the Pleistocene prior to this Buckland glaciation. Sediments were typically thick beds of gravel with interbedded sands. It was into this setting that glaciers infringed. Refer to **Appendix A** for Quaternary geology map of Yukon Coastal Plain.

The Buckland glaciation, during the Early Wisconsin, affected the Yukon Coastal Plain (Rampton 1982). This era corresponds to 120– 75 Ka and Oxygen Isotope (IS) stage 5 (Rampton 1982). Other documented minor glacial advances include the Sabine phase advance of the Buckland glaciation that corresponds to Oxygen Isotope stage 2 (25 – 10 Ka) (Rampton 1982). This phase likely occurred after the apex of the ice limit and may have not directly scoured the Yukon coastal plain but may have, deposited long morainic ridges and outwash channels/gullies onto the plain (Rampton 1982). All Pre-Buckland sediments pre-date the early Wisconsin.

Dissected meltwater channels are also common (Rampton 1982). Alluvial fans with distal edges are frequently overlain by glacial deposits attributed to the Buckland glaciation (Rampton 1982).

Thermokarst activity was initiated after deglaciation in the post glacial era and substantially shaped local topography. Thermokarst basins formed actively between 12-8 Ka (Rampton 1982). Moraine relief is largely due to thermokarst terrain. West of Shingle Point are fine grained marine, deltaic and floodplain sediments (Rampton 1982). The area east of Shingle Point Quaternary sediments has sands, gravels interbedded with sand, silt, and further oxidized gravel (Rampton 1982). Oxidized till is abundant along the Running River. Significant debris flow events, typically of lacustrine or colluvial deposits, are related to the initiation of thaw cycles in the post-glacial time (Rampton 1982).

In the modern setting, the landscapes' glacial reworking is visible with ground, rolling and hummocky moraines left behind (Rampton 1982). Interbedded silt, wood and organic detritus are main constituents of the till and sometimes gradationally overly marine sediments that pre-date the Buckland glaciation (Rampton 1982). Lower oxidized gravels represent an alluvial fan or terrace deposit under conditions cold enough to allow ice wedges to form (Rampton 1982). Following their deposition, the climate presumably warmed up enough to a point where ice wedges thawed and gravels oxidized to depth implying a significant degradation of permafrost (Rampton 1982). Oxidization of sediments exposed in Blow River sections further support this inference.

Dated fossil evidence suggests that the post-Buckland landscape was tundra shaped by fluvial landforms and deposits, thermokarst, mass wasting events (i.e. thaw lakes), and the

formation of ground ice. Macrofossil, pollen evidence, and thermokarst chronology indicate a climatic warming shortly after 11 Ka (Rampton 1982). It is in this setting that Arctic drainage networks evolve.

4.4.0: Quaternary Climate

Climate change through the Holocene and Pleistocene epochs has significant consequences for topography and vegetation in the modern Yukon coastal plain. References to Pliocene climate change will also be addressed. Palynological and faunal evidence has been used to reconstruct past climates.

Pliocene climate trends are generalized as a warm period with intermittent cold spikes (White 1997). Uplift during the late Pliocene warm period had little effect on the climate in the Yukon coastal plain. The opening of the Bering Strait around 3 Ma, which had previously been a barrier between Arctic and Pacific Ocean since the Cretaceous, is speculated to be the source of this warm period (White 1997). Although heat transfer through the Bering Strait is a small component of the Arctic heat Budget, the event likely warmed and moderated the Arctic Ocean (White 1997).

The Pleistocene was notably colder than the Pliocene epoch. The occurrence of *Criboelphidium ulstulatum* foraminifera, thermophilus taxa (*Fagus* and *Quercus*), in most cores at this time, indicates the frigidness of the local Arctic waters (White 1997). Decreased forest canopy and decreased paludification is recorded during this interval (White 1997). Climatic continentality and dryness may explain the abundant increase of *Cyperaceae* and *Sphagnum* after

3 Ma (White 1997). Thicker more persistent permafrost occurred as the glacial cycle deepened in the late Pleistocene (White 1997).

The Holocene is characterized by a general warming trend after the Pleistocene “deep freeze”, with intermittent cold spells (Vardy *et al.* 1997). High levels of *Picea* pollen in the early Holocene indicate tree line was 75-100 km north of its present limit (Vardy *et al.* 1997). *Larix laricina* tree stump from peat deposits show that the range in this species extended 75-80 km beyond its present limit (Vardy *et al.* 1997). These two instances generally allude to a warmer climate then than at present. An example is the dominance of the Dwarf Birch from 11-7 Ka Macrofossil, pollen evidence, and thermokarst chronologies indicate a climactic warming shortly after 11 Ka (Rampton 1982). This warmer climate may be a result of early Holocene Milankovitch insolation maximum (White 1997). Sea level is also suspected to be lower than today (Vardy *et al.* 1997). *Picea mariana* in the Mackenzie Delta estimate mid-summer temperatures to be three degrees warmer than today (Vardy *et al.* 1997). Climatic degradation began ca. 8000 B.P (sidereal age) with rapid cooling ca 4500-5000 B.P from paleoecological record from lake sites (Vardy *et al.* 1997). Late Holocene cooling in the Arctic has been linked to changes in North Atlantic circulation (Miller 2001). At 6300 B.P permafrost and ice began to form in Arctic Regions (Vardy *et al.* 1997). By 4700 B.P low centered polygons developed and eventually evolved into the high centered polygons seen today (Vardy *et al.* 1997).

4.5.0: Recent Climate

Climate of the Yukon

Coastal plain is cold and arid with sub-zero winter time conditions prevailing for an average of 250 days of the year (Rampton 1982). I compiled climatic data for the past 50 years from the DEW point weather station on the Yukon coastal plain from

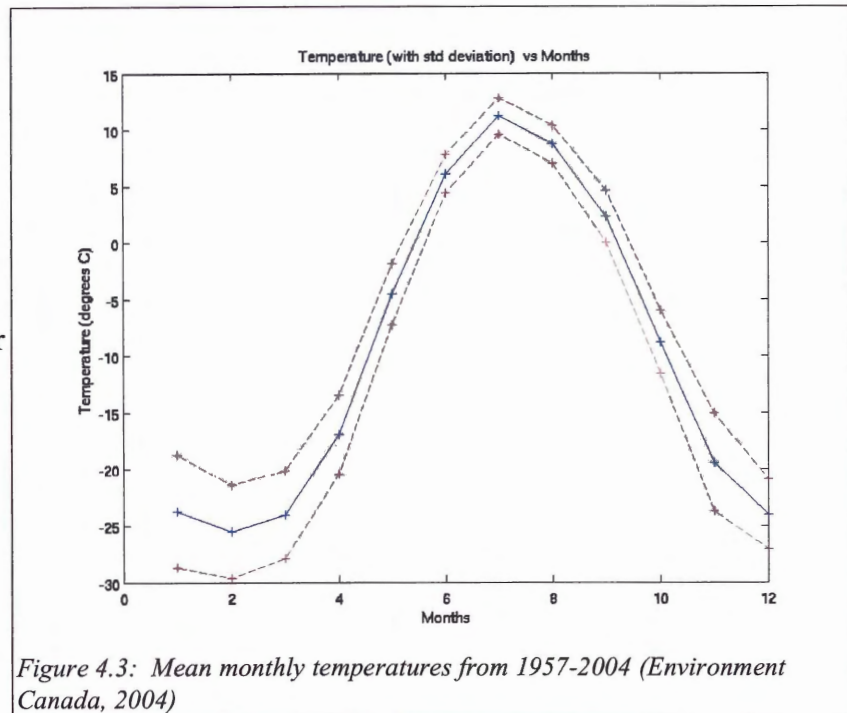


Figure 4.3: Mean monthly temperatures from 1957-2004 (Environment Canada, 2004)

Environment Canada Climate Data (Environment Canada 2004). Averages for each month are displayed in Figures 4.3-4.6. Figure 4.3 shows the annual distribution of sub-zero temperatures for virtually nine months of the year. The spring melt occurs during June and July. During the winter months (September through unto the end of May) cold continental air dominates the system, whereas in the summer months (July and August), warm maritime air dictates the local weather.

Snow fall in the region averages 50 cm annually (Rampton 1982). Figure 4.4 illustrates the maximum rainfall of approximately 53 mm occurs during the wet month of August. Compared to low latitude, temperate regions, this value is low (Section 4.6.0).

Figure 4.4 depicts the low annual precipitation, with a maximum of 55 mm occurring during the wet month of August. Year round precipitation values hover around 8 mm, and rainfall turns to snowfall during mid-late October. Once snow has fallen onto the coastal plain, cold

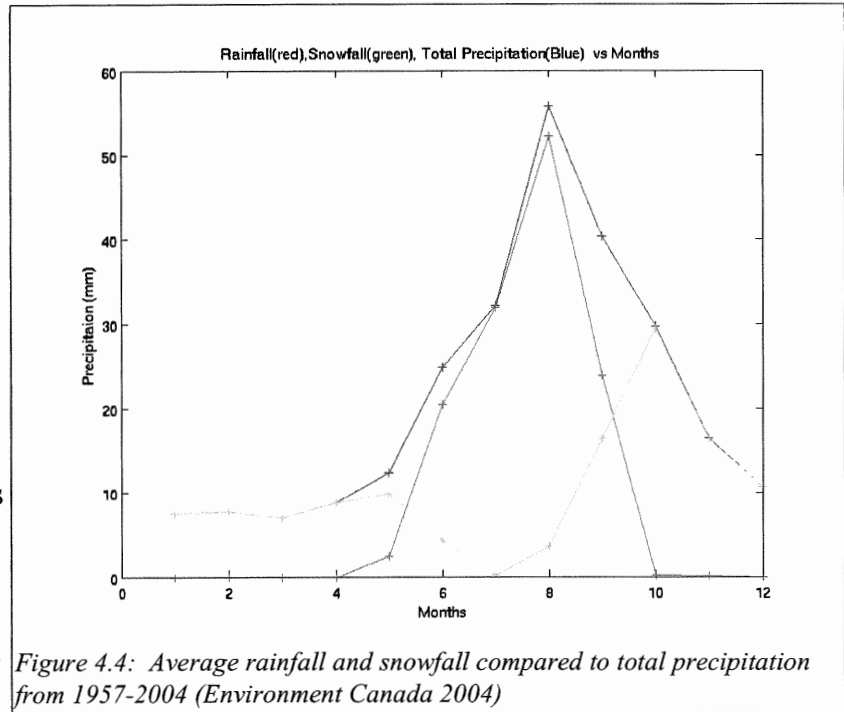


Figure 4.4: Average rainfall and snowfall compared to total precipitation from 1957-2004 (Environment Canada 2004)

winter temperatures allow the snow to remain all winter.

Figure 4.5 displays the minimal amounts of snowfall and snow accumulations year round. Noticeably, snow ground cover may persist almost all year with the exception of around two weeks in mid July, which correspond to the highest average annual temperature

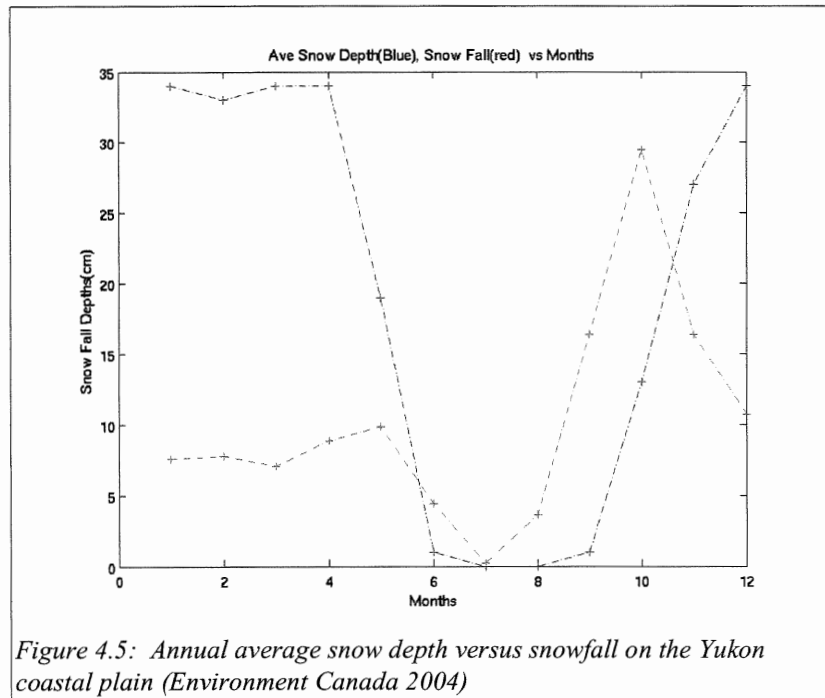


Figure 4.5: Annual average snow depth versus snowfall on the Yukon coastal plain (Environment Canada 2004)

(Fig. 4.3). Snow that falls persists until the melt season (June), isolating and insulating the peat and permafrost.

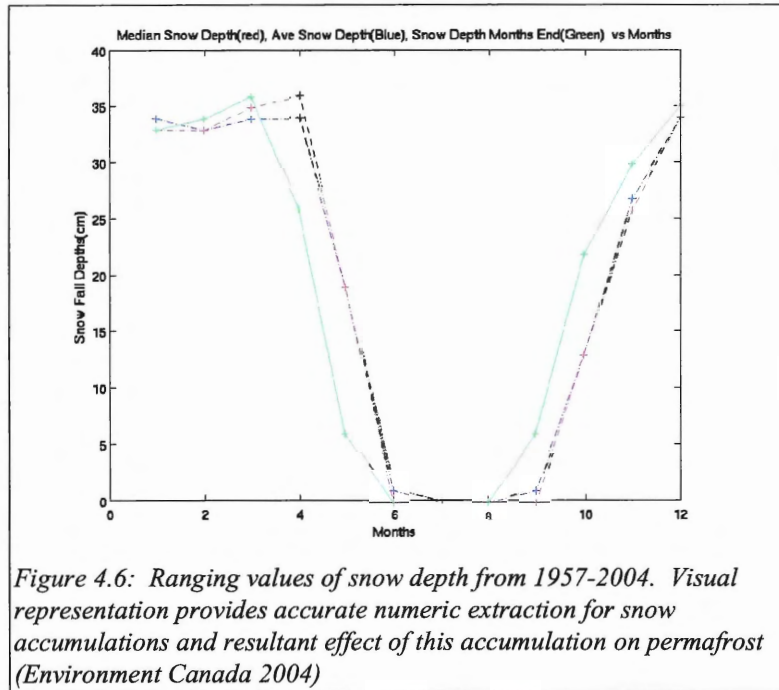


Figure 4.6: Ranging values of snow depth from 1957-2004. Visual representation provides accurate numeric extraction for snow accumulations and resultant effect of this accumulation on permafrost (Environment Canada 2004)

During winter months (Late September – Late June), the average maximum snow depth of 33 cm is reached in April (Fig 4.6). Snow cover extent in the Arctic has decreased 10% in the last 30 years (Fig. 4.7) (Hassol 2004). In areas of the Alaskan Arctic, snow cover end date has shifted to one month earlier in the last 50 years (Hassol 2004).

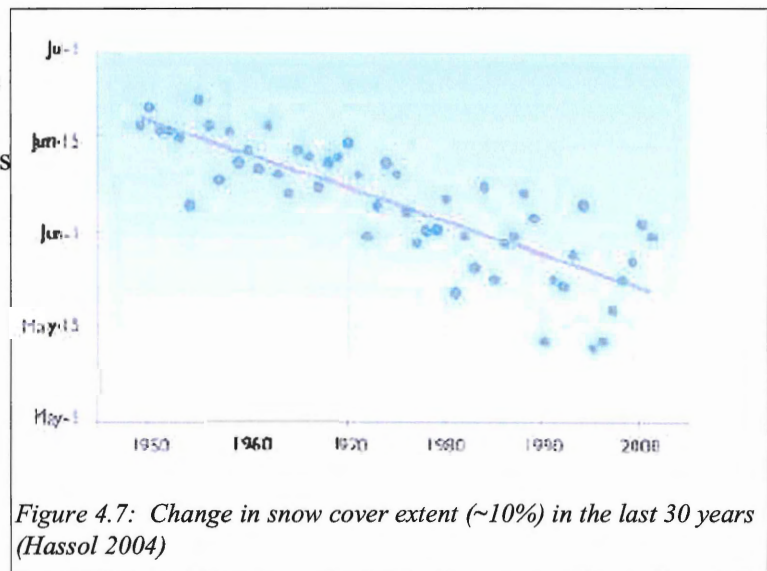
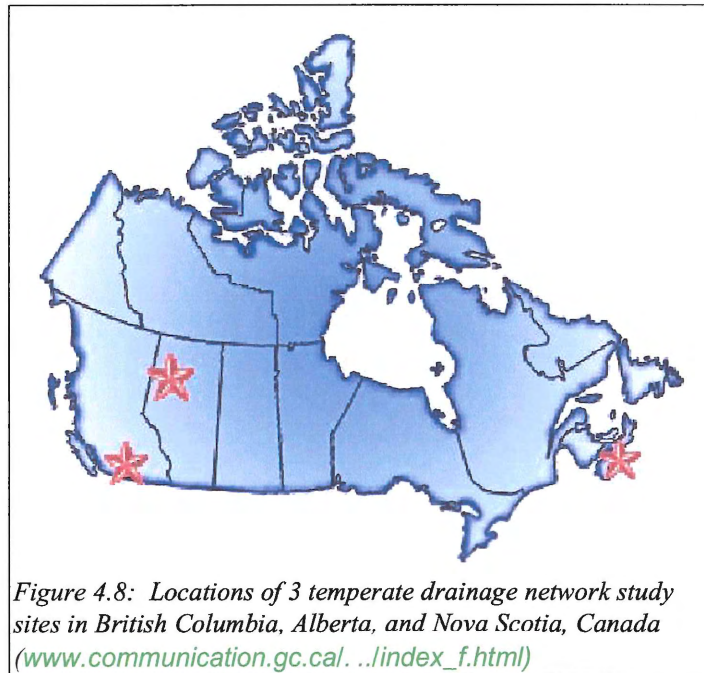


Figure 4.7: Change in snow cover extent (~10%) in the last 30 years (Hassol 2004)

4.6.0: Temperate Study Locations



Arctic drainage networks attributes are comparatively tested against 3 locations of lower latitude, temperate nature (**Fig. 4.8**). These networks provide accurate values to test my methodology by comparing my temperate results against published parameters. The 3 temperate sites are the Keg River of northern Alberta, Nicklen Creek of south central British Columbia, and the East River of coastal Nova Scotia. Attributes of these areas are:

River	River Origin Location (Longitude/Latitude)	Mean Annual Temperature (°C)	Mean Annual Precipitation (mm)
Keg River (AB)	117.57917 57.747500	1.2 ± 12.1	33.5 ± 20.4
Nicklen Creek (B.C.)	119.14000 50.076667	9.0 ± 8.2	28.3 ± 5.5
East River (NS)	62.259167 45.110000	7.7 ± 8.6	125.7 ± 20.8

Table 4.1: Attributes of temperate study sites (Environment Canada 2004)

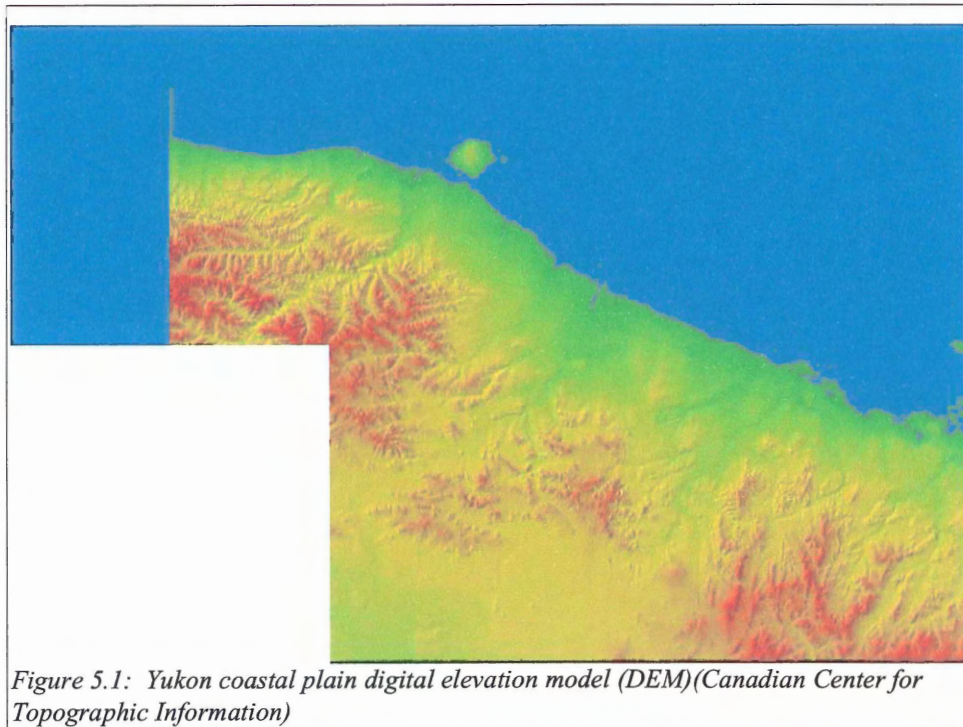
Chapter 5.0.0 Methods

5.1.0: General Approach

Analysis using newly introduced DEM data has made analysis of large drainage basins possible and statistical acquisition of these basins accurate (Rodriguez-Iturbe and Rinaldo 1997). Prior to this, field data and measurements were the limited data acquisition and analysis method. The combination of field work with accurately measured DEM data allows dependable data extraction with human observations as a data audit.

5.2.0: Digital Elevation Models (DEMs)

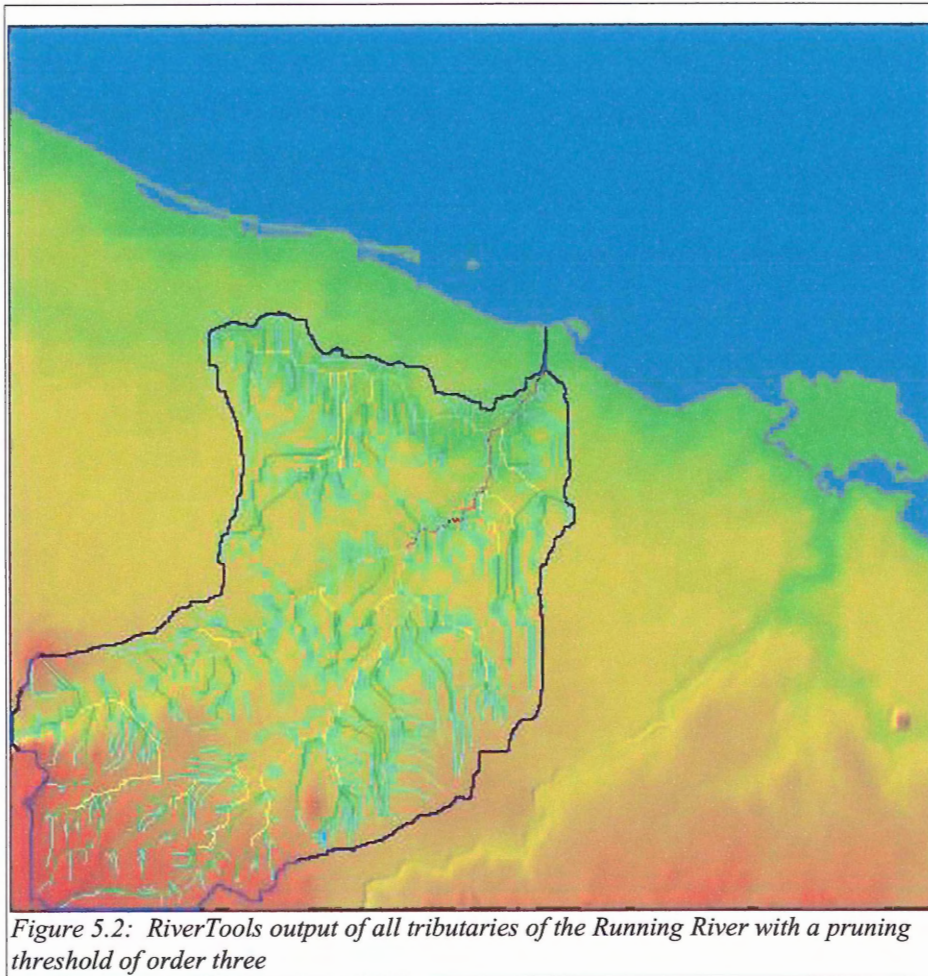
Regularly spaced grid cells compose the data structure of DEMs. In such a grid, elevations are available as a matrix of points equally spaced in two orthogonal directions



(Rodriguez-Iturbe and Rinaldo and Rinaldo 1997). Spacing in DEMs used in this study have an order of 90 m resolution. Mean vertical resolution for these DEMs is 2.3 m (**Appendix E**). Each grid block with the DEM is called a pixel and RiverTools uses elevations associated to each pixel to assign a drainage direction from each pixel to one of its eight neighbours (**Section 6.40**).

5.2.1: Digital Elevation Model Acquisition

I used digital elevation models from Geobase, a federal, provincial and territorial government initiative overseen by the Canadian Council on Geomatics (CCOG). Files are Canadian Digital Elevation Data (CDED) in a U.S Geologic Survey (USGS) format. CDEDs consists of an ordered array of ground elevations at regularly spaced intervals. The source digital data for CDED at a scale of 1:250 000 are extracted from hypsographic and hydrographic measurements of the National Topographic Data Base (NTDB) and scaled positional data acquired from the provinces and territories. CDED files contain a Western and an Eastern section corresponding to half an National Topographic System (NTS) map sheet. Depending on specified latitudes of the CDED section, grid spacing for the 1:250 000 NTS tiles ranges from 3 to 12 arcs seconds. Ground Elevations are recorded in meters relative to Mean Sea Level (MSL), based on the North American Datum 1983 (NAD83) horizontal reference datum. CDED provide values of elevation points (accuracy is resolution specific), orientations and slopes of each point. Numerous DEMs are merged together in RiverTools to allow a larger area to be analyzed. From this, selected areas are isolated and saved as an additional DEM from which results are extracted.



5.3.0: Drainage Network Analysis

Prior to analysis, digital elevation models were imported from CDED into the *.rtg* RiverTools format and merged as needed (**Fig. 5.1**). RiverTools uses DEMs to produce maps, but also to make measurements and to derive quantitative information on drainage basins. Examples of quantitative measurements include the lengths and slopes of channel segments, contributive area of a watershed, the number of streams of a given order, the shape of a longitudinal profile, a basin's hypsometric curve, and basin shape.

I then used RiverTools to extract a D8 flowgrid from the DEM. Flow direction from every pixel in the DEM to one of its eight neighbouring pixels is calculated from local slope and stored in a grid that has the same dimensions as the DEM. Each element in this grid contains a “flow code” that is a numerical pointer for one of the eight primary compass directions. The drainage network – formed by interconnected flowpaths – is then extracted by specifying its drainage outlet. For example, the Running River mouth is selected, and all flow paths that lead to this outlet comprise its drainage network.

RiverTools provides a complete drainage network in which essentially all pixels are channels. A user-defined pruning threshold is then used to eliminate the lowest order “channels” from this network. The user specifies a threshold that removes channels from the modeled network which do not occur in nature. The selection of this pruning threshold is a key aspect of analysis, and is addressed later.

Once the network has been extracted, it can be viewed in various ways. Shaded relief is generated by projecting light onto the DEM from a given azimuth to enhance topographic features. River network display shows drainage networks (defined as order by pruning) of the chosen watershed. Plots can be combined into multiple layers on one figure. I plotted drainage area, along channel length, and along channel slope against Strahler stream orders and took values of R_B , R_L , R_A , and R_G from the RiverTools summary data for each basin.

5.4.0: Air Photo Inspection

Aerial photographs provide one method of checking RiverTools' extraction of drainage networks, especially “pruning” of Horton-Strahler stream orders. In pruning the lowest stream

orders are removed from the network because they do not occur in natural networks. RiverTools uses elevations of pixels in DEMs to determine flow paths and, without pruning, interprets all flow paths as open water channels. I compared channels, including water tracks, visible in 1:20,000 scale aerial photographs to flow paths in RiverTools flow grid, and pruned until the remaining channels correspond to channels visible on the landscape. Numerous pruning thresholds 0-4 were used to determine the threshold that reproduced the observed pattern. The

best-fit pruning occurs at a threshold of 3 because no channels are visible on air photos below this threshold. Order 4 pruning eliminates major water tracks and is therefore unacceptable. After pruning the Strahler stream orders are re-numbered so the remaining lowest order channels are order 1.

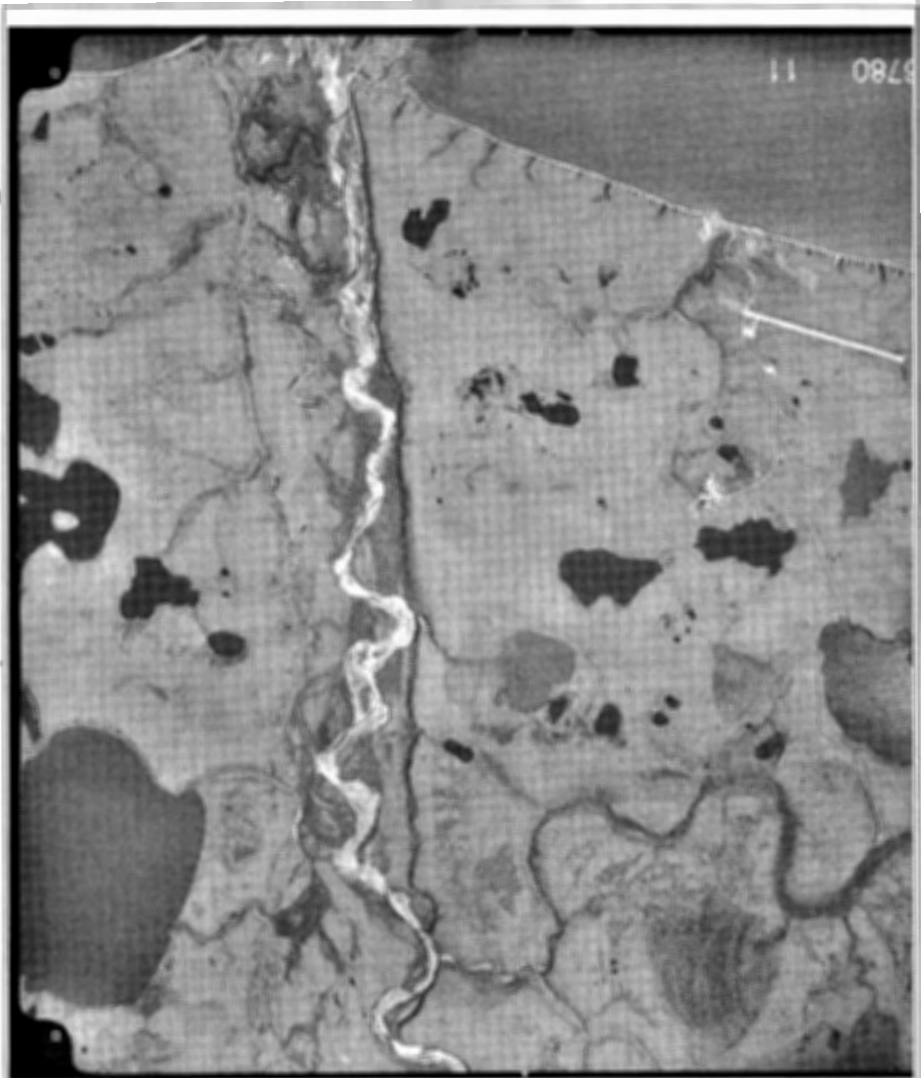
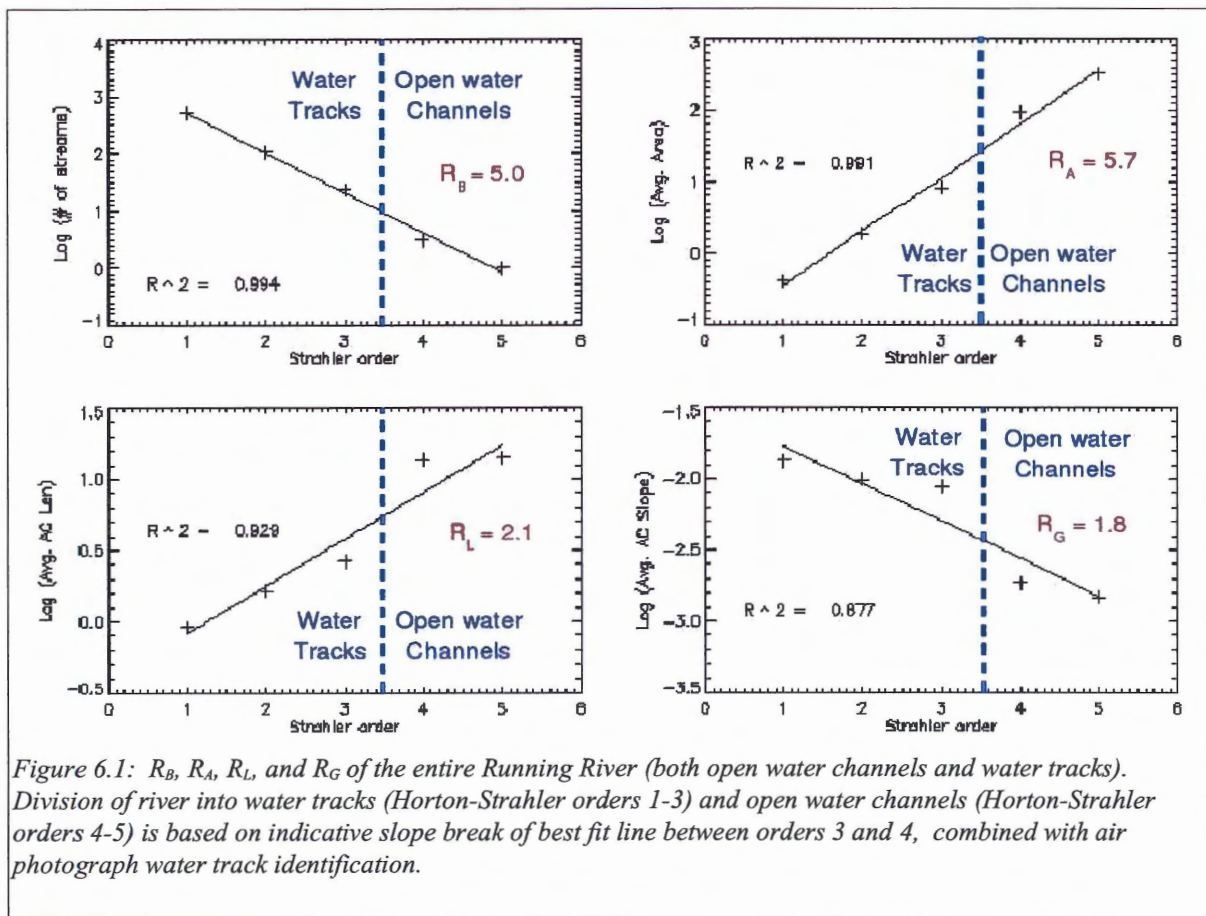


Figure 5.3: 1985 Air photograph of the Yukon coastal plain. The central river is my study area, the Running River. The large water body at the top of the picture is the Beaufort Sea

Chapter 6.0.0: Results and Discussion

Statistical properties of drainage networks, including Horton laws such as bifurcation length, area and gradient ratios, commonly are used to quantify network properties. They may also be used to compare between networks, and probe for differences that reflect underlying fluvial processes and geology. In this chapter I use R_B , R_L , R_A , R_G to show such differences.

6.1.0: Bifurcation (R_B), area (R_A), length (R_L), and channel gradient (R_G) ratios in the Running River Drainage Basin

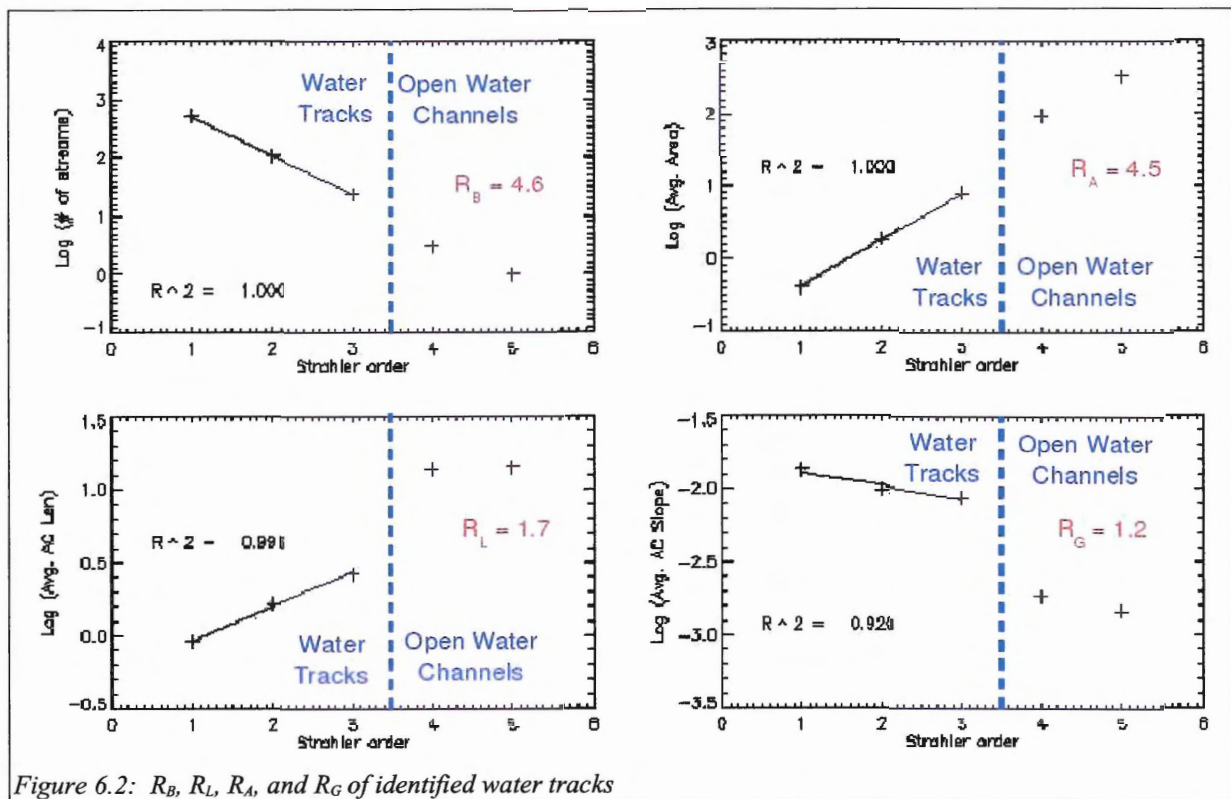


6.1.1: All Channels

The Running River has bifurcation ratio 5.0, area ratio 5.7, length ratio 2.1, and channel gradient ratio of 1.8 (**Fig. 6.1**). The straight line fit for bifurcation and area ratios are strong, with R^2 values of 0.994 and 0.991 respectively. The data fit for length and gradient ratios are less but remain statistically significant, with R^2 values at 0.929 and 0.877 respectively. These results suggest, at first glance, that the Running River basin follows Hortons' Law of Stream Orders over all scales.

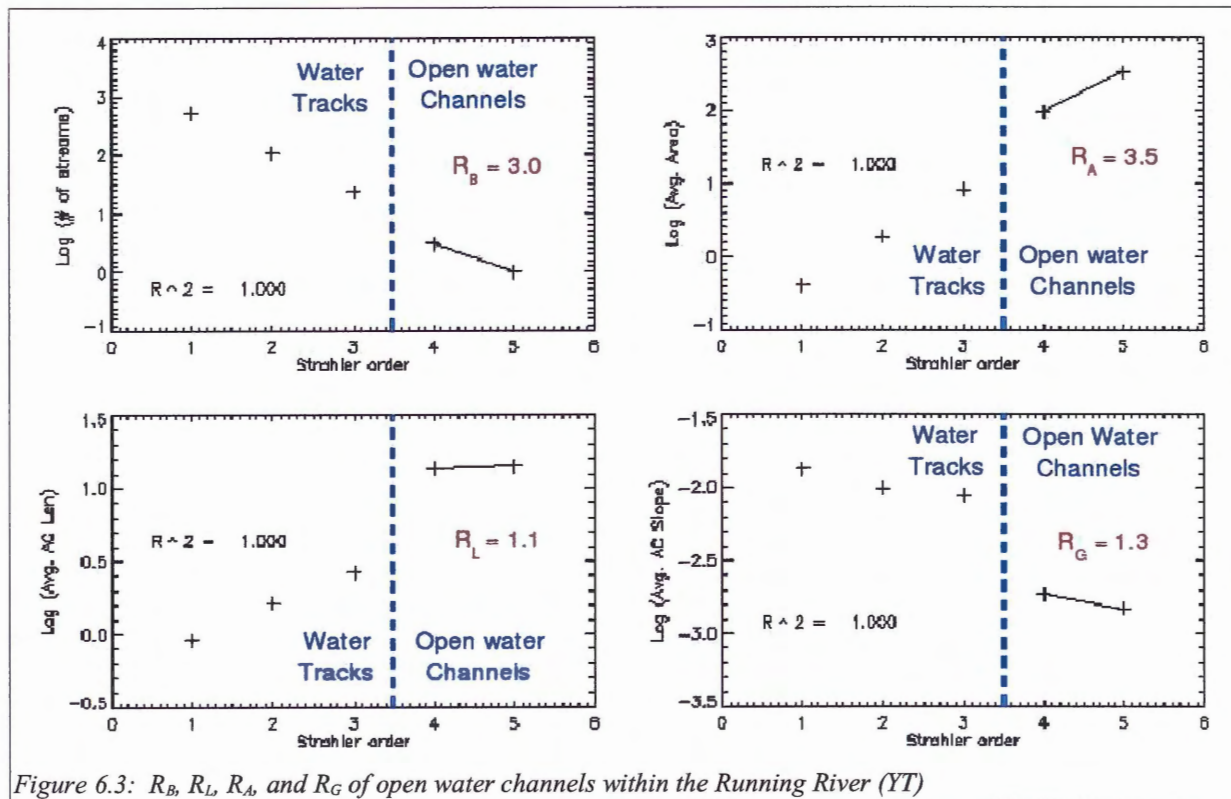
Despite the fit across all orders, inspection of results and the relatively low R^2 values for length and gradient ratios suggests, the Running River network displays a break in geometric scaling between stream order 3 and 4. This slope break also exists for bifurcation and area ratios, but is less pronounced. To explore this break in slope, analysis of the network was divided into two classes: up to and including order 3, corresponding to water tracks, and above order 3, corresponding to open water channels (**Fig. 6.2 and 6.3**).

6.1.2: Channels Below Order 3



Bifurcation, area, length, and gradient ratios of the entire Running River were 5.0, 5.7, 2.1, and 1.8 respectively, and R^2 improves when calculated only for low order streams (Fig. 6.1). Specific values for isolated water tracks include a bifurcation ratio of 4.6, area ratio of 4.5, length ratio of 1.7 and a gradient ratio of 1.2 (Fig. 6.2). Compared to basin-wide values, an overall reduction of ratios occurs in low order channels. Again, the definitive slope break is pronounced in Fig 6.2.

6.1.3: Open Water Channels



Isolation of open water channel ratios again provide another range of values. This is expected due to the different behaviour (i.e. flow regime) associated to open water channels. Generally, further depressed ratios as compared to **Figure s 6.1** and **6.2** are observed. Bifurcation, area, length ratios have decrease by 65%, 79%, and 61% respectively (**Fig. 6.3**). Channel gradient ratio remains approximately constant at 1.3 within open water channels, but a sharp break between order 3 and 4. A perfect data fit for the data occurred with R^2 values of 1.00 for all four ratios. This is expected due to only two points (4th and 5th order channels) existing for this section of the Running river and are therefore not actual R^2 values. If a 6th order channel existed in my study area, a less accurate R^2 value would likely result. The 3rd to 4th order slope

break is again observed in **Figure 6.3** when these Horton plots are segmented into water tracks and open water channels.

6.1.4: Comparison with Temperate Networks

	Temperate Networks (Global Averages)	Temperate Networks (this study)	Running River – Entire River	Running River – Open Water Channels Only	Running River – Water Tracks Only
Bifurcation Ratios (R_B)	3.7 ± 0.2	3.9 ± 0.3	5.0	3.0	4.6
Length Ratios (R_L)	2.6 ± 0.1	1.9 ± 0.2	2.1	1.1	1.7
Area Ratios (R_A)	4.5 ± 0.3	4.3 ± 0.2	5.7	3.5	4.5
Gradient Ratios (R_G)	N/A	1.3 ± 0.2	1.8	1.3	1.2

Table 6.1: Comparative results Arctic network ratios to temperate study ratios. Global averages are reported from 6152 networks across Africa, Asia, Australia, Europe, North America, and South America (Vorsomarty 2000). Independent measurements using fewer networks but higher resolution DEMs show similar areas (Ignacio-Iturbe 1997)

Drainage networks have been proposed to be scale invariant, a hypothesis consistent with many previous published measurements of network characteristics (Ignacio-Iturbe 1997). This scale invariance may occur across geologic and climatic conditions (Ignacio-Iturbe 1997). However, my results show that Running River network properties show a distinct break in scaling after order 3. This is shown by **Figures 6.1, 6.2, and 6.3**, and by comparison of R_B , R_L and R_A with global average values (**Table 6.1**). The temperate networks I analyzed fall, however, within global average, suggesting the methodology I employed is sound.

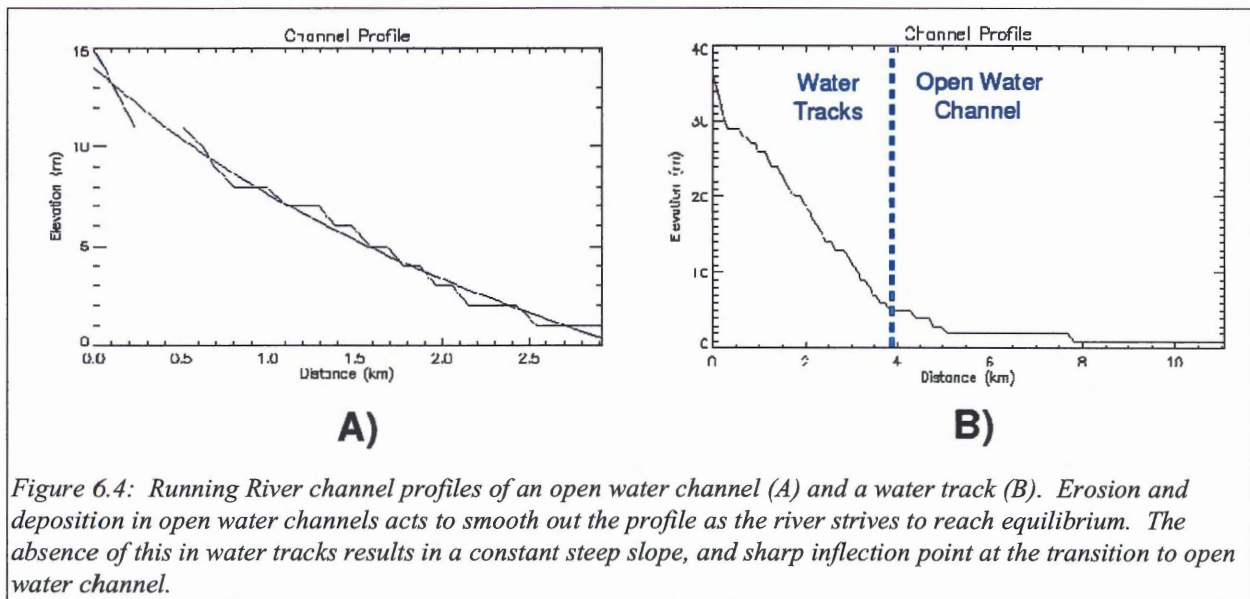
Similar bifurcation ratios (**Table 6.1**) between global (3.7 ± 0.2) and my temperate networks (3.9 ± 0.3) are shown in **Table 6.1**. The bifurcation ratio of the entire Running River shows is elevated (5.0) compared to the temperate networks. This ratio remains high for only water tracks (4.6) but drops off dramatically when isolating open water channels (3.0), although the significance of the open water value for the Running River is questionable because it is calculated across only 2 orders of channels. This difference in ratios denotes a more branching (bifurcated) nature to water tracks compared to Arctic open water channels and globally averaged networks.

A more pronounced difference exists in the length ratio comparison (**Table 6.1**) within temperate networks. Noticeable differences of Arctic networks include a lower length ratio of water tracks (1.7) as compared to both my temperate drainage networks (1.9 ± 0.2) and the entire Running River (2.1). Channel lengths do not increase through 1st, 2nd, and 3rd order water tracks as rapidly as they do in similarly ordered streams of temperate networks. R_L also is small for the Running River when calculated across only the 4th and 5th order open water channels. This is also observed for the East River study area in Nova Scotia (Appendix D). The probable cause of the shortening of the high order channels is landward coastal erosion independent of, or combined with, local sea level change.

Despite different branching and channel lengthening behaviour for low order Running River channels (water tracks), R_A is comparable to temperate networks. Similar area ratios are observed (**Table 6.1**) across global (4.5 ± 0.3), my temperate (4.3 ± 0.2) and water tracks of the Arctic (4.5). These results show that water tracks drain similar areas as temperate low order

channels, but may do so through a different geometry (heavily branched, constantly long). A potential feedback loop exists between the low length ratio and high bifurcation ratio water tracks that finds common ground in similar area ratios. The elevated area ratio of the entire Running river (5.7) is plausible but likely just an expression of the slope break seen on all Horton plots and the inaccurate data fit in this circumstance. The low area ratio of open water channels (3.5) can again be attributed to coastal headward erosion and local sea level changes diminishing the Running Rivers' drainage basins.

The channel gradient ratio for global networks is not depicted in **Table 6.1** as this ratio is not common to published work. The significance of this ratio is noted in that water tracks ratio (1.2) is lower than that of open water channels (1.3) (**Figs. 6.2 and 6.3**). Water tracks slope is therefore changing less/order than open water channels. A steep, constant profile is observed in water tracks of the Running River whereas open water channels in the Running river resemble the smooth, concave upward profiles found in temperate networks (**Fig. 6.4**).



6.2.0: Critical Basin Areas

Comparative analysis of the minimum drainage basin area required (critical basin area) in order to initiate open water channels versus water tracks gives insight into the potential conditions required for the evolution of water tracks into open water channels. Water tracks critical basin area is $0.1 \pm 0.9 \text{ km}^2$ whereas high order, open water channels critical basin area is $11. \pm 9.7 \text{ km}^2$. Calculations of these critical basin area are found in **Appendix E**.

6.3.0: Discussion

Compared to temperate networks, the Running Rivers' drainage network has elevated bifurcation, and reduced length ratios. My hypothesis is these can be accounted for by unique processes operating within Arctic water tracks, namely the lack of incision, erosion and deposition due to different hydraulic flow regimes. The presence of these drainage pathways is well documented in published data and my ratio values are quantitative expressions of such structures.

In this Arctic setting, a very permeable (hydraulic conductivity 10^{-3} ms^{-1}) (Chason and Siegel 1986), minimally decomposed (fibric) layer (~0.4 m thickness) of Carex peat rests on top of a continuous, impermeable (hydraulic conductivity of 10^{-13} ms^{-1}) (Norris 1996) permafrost layer. This peat is very capable of accepting the minimal amounts of precipitation (spring runoff combined with minimal annual precipitation) (**Section 2.5.0**) introduced to the system. As a result of this permeability contrast, water flow is restricted to the active layer on top of the permafrost table, with the water table being isolated by the continuous permafrost. Flow through peat is generally laminar (Quinton *et al.* 2000). Laminar flows have virtually no erosive power

(Leopold *et al.* 1992), and intact fibric peat forms a mat resistant to entrainment. Because of high permeability, water levels never overwhelm this porous medium and overland flow above the peat layer does not occur. This prohibits erosion, and the “channel” can not incise. In contrast, temperate networks lack this permeable buffer and therefore turbulent, overland flow is common during precipitation events, with resulting erosion, incision of channels (silty soils have permeability 10^{-9} - 10^{-6} m/s compared to 10^{-4} m/s for fibric peat) (Freeze and Cherry 1979). Field observations, the lack of open water channels, and the absence of well define hydrologically sourced topographic depressions support this view. The lower gradient ratio further supports the lack of incision. In temperate systems, low order streams above divides adjust their own gradients by incision, and the

longitudinal profile is smoothed by downstream deposition (**Fig. 6.5**).

The inverse occurs in the Arctic where low order streams (water tracks) have gradients that change very little downstream in higher order channels

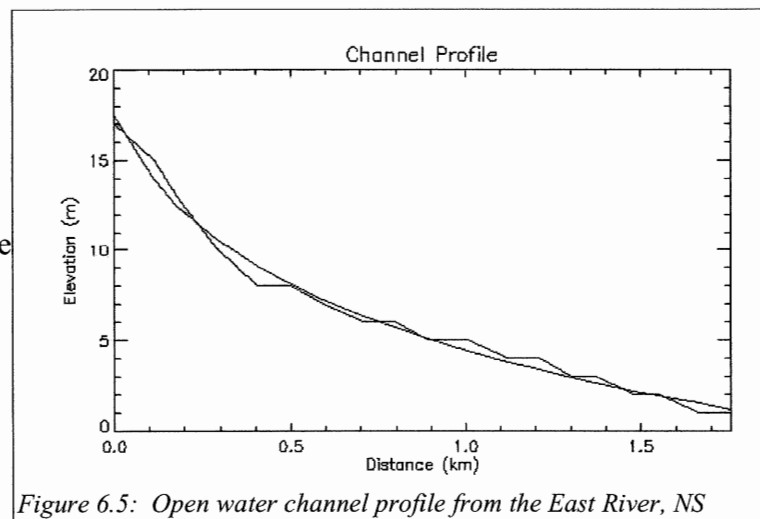


Figure 6.5: Open water channel profile from the East River, NS

– until open water channels are reached (**Fig. 6.4**). Erosion is observed in these open water channels with minor sediment fans seen being expelled into the Beaufort Sea.

The elevated bifurcation ratio in the Arctic also is explained by non-erosive, laminar flow regime in water tracks. Because no incision occurs, water tracks simplistically transport water down fall lines. In temperate networks, incision occurs into the substrate due to overland,

turbulent flow, producing small channels (rills) which incise and induce cross-grading. This draws in drainage from surrounding areas, centralizing drainage into “gutter like” pathways that pirate other adjacent channels (**Fig. 6.6**). The result is less branching of tributaries into main rivers as larger, open water networks are a more efficient way of draining the watershed if precipitation amounts permit. In the Arctic, lowering of bifurcation by cross grading does not occur due to the lack of incision. Drainage channels cannot draw in other channels like water “tractor beams”, and flow over permafrost is free to branch independent of neighboring networks (**Fig. 6.6**). Possible altering factors in the Arctic include; vegetative differences in the peat causing porosity irregularities, and permafrost table depth differences. Both of these may have a significant impact on the flow regime and the possibility of achieving overland flow.

The low length ratio for the Running River also is explained by suppression of incision in water tracks. First order water tracks can flow alongside one another indefinitely because cross-grading does not occur. There is no cannibalization of water tracks by surrounding channels as they never drain into each other.

The similar area ratio is a result of no incision balancing out the high branching rate and the low lengthening ratio. Constantly long, branched networks can drain similar areas but through a different geometry. Typically an oval like curve is drawn around typical temperate drainage basins with regular branching within this boundary. Arctic networks planar profile would resemble an elongated rectangle with long, tentacle like channels within this boundary. Fractal space filling (**Equation 5**) is not accomplished in the Arctic setting due to this unique

geometry and is supported by an elevated D_{EL} value of 2.8 in contrast to a value of 2.0 for a space filling fractal.

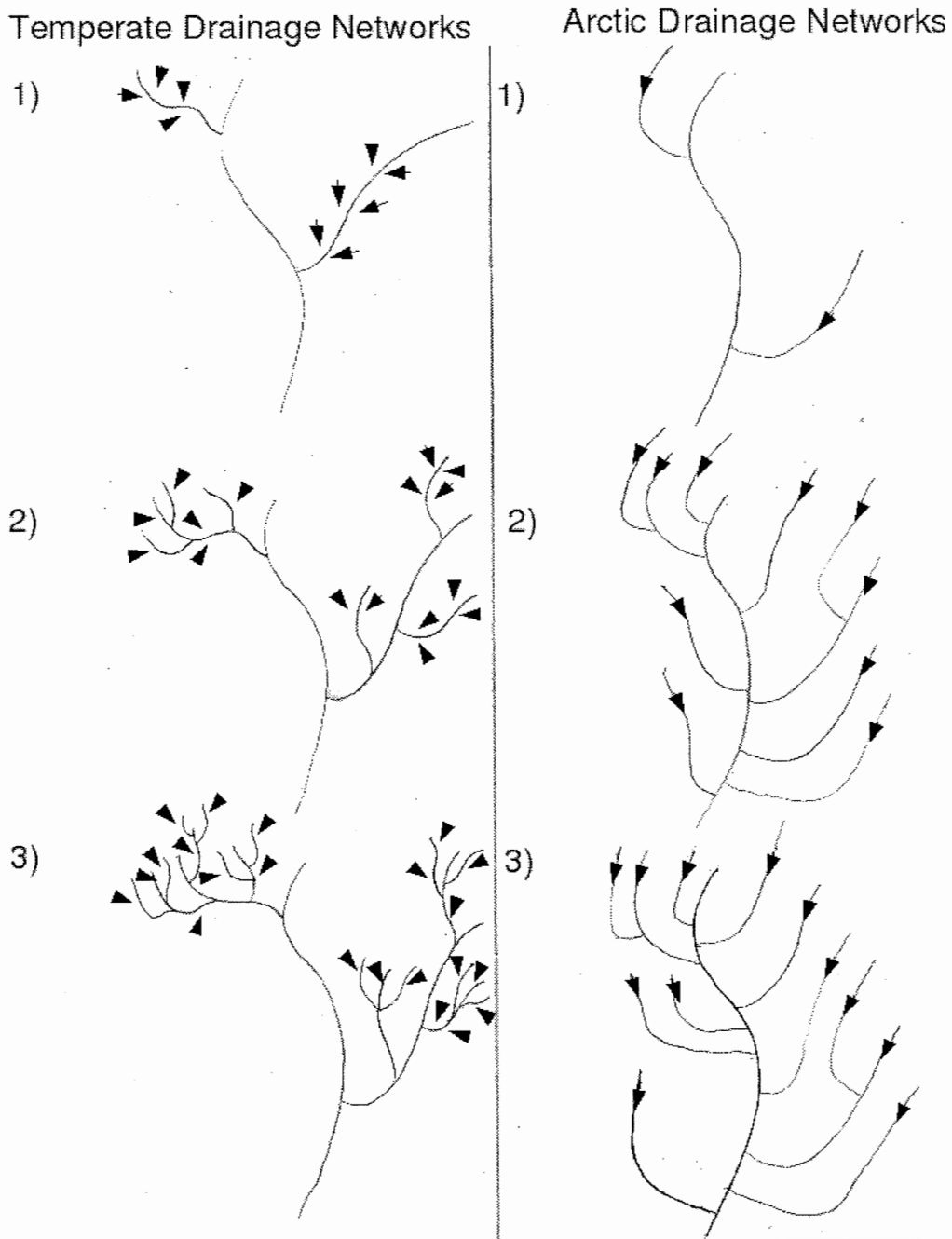


Figure 6.6: Evolution of Temperate and Arctic networks. Arrows denote hillslope flow paths. Variable directions in temperate networks are a result of active incision creating regional lows which pirate water from surrounding channels. Incision is not occurring in Arctic water tracks therefore channels are not drawing water from each other.

6.3.1: Causes of Open Water Channels on the Yukon Coastal Plain

Water tracks are not the only drainage mechanism for water shed drainage on the Yukon Coastal plain. Incised, open water channels occur where the porous peat medium has been overwhelmed at some point in time. One explanation is that these channels initiate during spring runoff events. Precipitation and spring runoff amounts (**Section 4.5.0**) are, however, meager to account for some large channel valleys (Gardner 2005). Observed field evidence shows underfit streams occupying these large channels during the wettest month of August. The next plausible explanation deals with the Glacial history of the area. Several high order, mountain sourced (Barn Mountains), incised rivers (Running River) have attributed origins as glacial outwash drainage networks, specifically the Buckland Glaciation during the Early Wisconsin (100-120 Ka) (**Section 4.3.0**). The Yukon coastal plain was free from effects from the last glacial maximum (20-24 Ka) being an isolated area between the Laurentide Ice sheet and the Western Cordillera. Many younger, intermediate order, open water channels exist on the landscape that are not sourced from adjacent mountain regions (Barn Mountains) and are too young to be associated to the Buckland glaciation. Channel initiation in this instance is attributed to catastrophic thaw lake drainage events overwhelming the peat medium and initiating open water channel incision. Water tracks are then forced into draining into these newly formed, topographic lows as is accounted for by field evidence and RiverTools outputs. Rapid channel initiation are intermediate steps in Arctic drainage networks evolution into mirroring temperate networks, with possible increase in thaw lake drainage accompanying global warming. With

longer summer seasons and warmer temperature, thaw lake evolution and drainage events are likely to become more numerous and possibly larger scale (Gardner 2005).

6.3.2: Effects of Anthropogenic Global Warming

At present, Arctic regions have experienced the greatest increase in annual mean temperatures, a trend predicted to continue throughout the next century (Hassol 2004). The thermal insulating properties of peat (**Section 3.3.1**) are not enough to shield underlying permafrost from this change in temperature. Associated with this increase in temperature are increased amounts of precipitation (Hassol 2004). Increased amounts of peat decomposition would likely accompany the increase in drier summer months. The amalgamation of these conditions may likely limit the peats ability in accommodating precipitation leading to it being overwhelmed by surface flow and overland, turbulent flow achieved. This may result in Arctic drainage networks evolving to mimic their temperate networks in overland, open water, incising flow.

Chapter 7.0.0: Conclusions and Future Work

Hillslope drainage on the Yukon Coastal plain is accomplished through small features labeled water tracks. Laminar hydraulic flow never overwhelms the very porous peat medium and therefore no overland flow is possible and river incision unlikely. Without cross grading and channel piracy, networks have unique quantitative expressions that differ from temperate drainage networks. The Arctic



Figure 7.1: A common willow tree as an analogy of the possible branching geometry of Arctic drainage networks

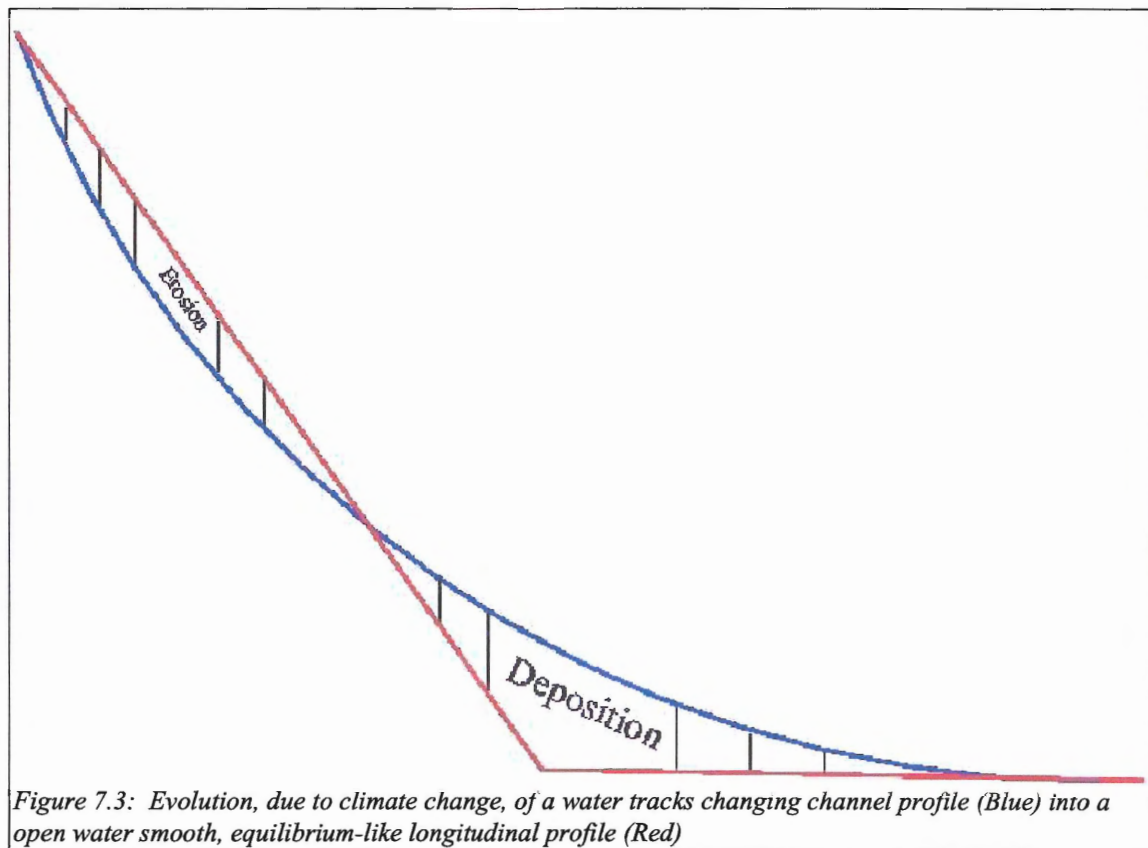
networks have highly bifurcated, constant length water tracks draining similar basin areas (**Fig 7.1**). The three orders of water tracks are not a true space filling fractal, as observed in temperate drainage networks (**Fig. 7.2**). Moreover, the sharp break in slope between water tracks and open water channels shows scale dependent properties in contrast to scale invariance proposed for



Figure 7.2: An oak tree as an analogue for the symmetrical, space filling (fractal) nature of temperate drainage networks

temperate networks without significant geologic controls. Open water channels do exist on this landscape. Many may be the result of short term lake drainage events overwhelming the porous peat medium. Climate change may amplify the overwhelming of the porous peat medium with increasing temperatures causing

permafrost reduction and hastening thaw lake margin expansion and number of drainage events, while increased precipitation inputs even more water into this finely balanced environment. These factors may force water tracks to be replaced by open water channels and exhibit a smooth, equilibrium-like longitudinal channel profiles (Fig. 7.3).



Quantitative expressions of water tracks influence on hillslope drainage need to be field tested and GPS surveyed to accurately pinpoint the exact geometry and behaviour of water tracks. Use of satellite imagery, comparison of annual aerial photographs, and ground surveys are required. Annual surveys of this landscape is also required in order to detail the evolution of

these networks and possible affects of global warming this area. Expansion of study areas into other terrestrial continuous permafrost terrains such as Siberia and Alaska, would help complete the global picture of Arctic drainage networks. Extraterrestrial application of this methodology to permafrost-rich Mars may provide a unique comparison of the permafrost-controlled break in fractal scaling on other planets. Analogue modeling using contrasting layers of permeability and cohesion may provide a step by step glimpse of water track evolution in permafrost terrains. The transition from water tracks to open water channels was not directly analyzed in this study, but is believed to contain many significant attributes associated to the break in fractal scaling. Processes that give rise to this transition require attention.

References

- Anderson, D.M., and Morgenstern, N.R. 1973. Physics, chemistry and mechanics of frozen ground. *In* 2nd International Conference U.S. Natural Academy Science Natural Resource Council. Washington, D.C.
- Ashmore, P., and Church, M. 2001. The impact of climate change on rivers and river processes in Canada. *Geologic Survey of Canada Bulletin*, **555**.
- Baird, A.J., and Heathwaite, L. 1997. Blanket Mire degradation: Causes, Consequences and Challenges. Macaulay Land Use Research Institute, Aberdeen.
- Boelter, D.H. 1969a. Physical properties of peat as related to degree of decomposition. *Soil society of America proceedings*, **33**: 606-609.
- Boelter, D.H. 1969b. Physical properties of peat as related to the degree of decomposition. *Soil society of America proceedings*, **33**: 606-609.
- Brown, R.J.E. 1966. Influence of vegetation on Permafrost. *In* Permafrost International Conference. *Edited by* N.A.o.f. Sci. Nat. Res. Council Publication, Vol.1287, pp. 20-50.
- Canadian Center for Topographic Information, <http://maps.nrcan.gc.ca> .
- Charman, D. 2002. Peatlands and Environmental Change. John Wiley and Sons Ltd., New York.
- Chason, D.B., and Siegel, D.I. 1986. Hydraulic conductivity and related physical properties properties of peat, Lost River peatland, northern Minnesota. *Soil Science*, **142**: 91-99.
- Cheng, Q., Russell, H., Sharpe, D., Kenny, F., and Qin, P. 2001. GIS-based statistical and fractal/multifractal analysis of surface stream patterns in the Oak Ridges Moraine. *Computer and Geosciences*, **27**: 513-526.
- Dyke, L.D. 1996. White, Barn, and Campbell Uplifts. *In* The Geology, Mineral and Hydrocarbon Potential of Northern Yukon Territory and North-western District of Mackenzie. Geological Survey of Canada, **Bulletin 422**. pp. 333-357.
- Environment Canada. 2004. Climate data of Shingle Point A (1957-2004). Environment Canada.
- French, H.M. 1996. The periglacial environment, Edinburgh.

- Gardner, D.W. 2005. Magnitude of Catastrophic Thaw Lake Drainage and Influence on Arctic River Channel Morphology, Yukon Coastal Plain, Western Canadian Arctic, Honours Thesis, pp.1-96.
- Hassol, H.A. 2004. Arctic Climate Impact Assessment: Impacts of a Warming Arctic. Press Syndicate of the University of Cambridge, Cambridge.
- Horton, R.E. 1945. Erosional development of stream and their drainage basins; Hydrophysical approach to quantitative morphology. *Geologic Society of America Bulletin*, **56**: 275-370.
- IPA. 2004. Global Permafrost Distribution. International Permafrost Association.
- Leopold, L.B., Wolman, M.G., and Miller, J.P. 1992. *Fluvial Processes in Geomorphology*. Dover Publications Inc., New York.
- Linell, K.A., and Tedrow, J.C.F. 1981. *Soil and permafrost surveys in the Arctic*. Clarendon press, Oxford.
- Mandelbrot, B.B. 1985. Self-affine fractals and fractal dimension. *Physica Scripta*, **32**: 257-260.
- McDonald, B.C., and Lewis, C.P. 1973. Geomorphic and sedimentologic processes of rivers and coast, Yukon Coastal Plain; environmental-social program, northern pipe-lines, Task force on Northern Oil Development, Terrain Sciences Division Geologic Survey of Canada.
- McNamara, J.P., Kane, D.L., and Hinzman, L.D. 1998. An analysis of an Arctic channel network using a digital elevation model. *Geomorphology*, **29**: 339-353.
- Miall, A.D. 1992. Alluvial Deposits. *In Facies Models*. Geological Association of Canada. pp. 119-143.
- Miller, G. 2001. Holocene paleoclimate data from the Arctic: testing models of global climate change. *Quaternary Science Reviews*, **20**: 1275-1287.
- Norris, D.K. 1996. Physiographic Setting. *In The Geology, Mineral and Hydrocarbon Potential of Northern Yukon Territory and North-western District of Mackenzie*. Geological Survey of Canada, **Bulletin 422**. pp. 7-19.
- Quinton, W.L., Gray, D.M., and Marsh, P. 2000. Subsurface drainage from hummock-covered hillslopes in the Arctic tundra. *Journal of Hydrology*, **237**: 113-125.

- Rampton, V.N. 1982. Quaternary Geology of the Yukon Coastal Plain. Geological Survey of Canada, **Bulletin 317**: 1-47.
- Ritter, D.F., Kochel, R.C., and Miller, J.R. 2002. Process Geomorphology. McGraw-Hill Higher Education, New York.
- Rodriguez-Iturbe, I., and Rinaldo, A. 1997. Fractal River Basins: Chance and self organization. Cambridge University Press, Cambridge.
- Rycroft, D.W., and Ingram, H.A.P. 1975. The transmission of water through peat. II Field experiments. *Journal of Ecology*, **63**: 557-568.
- Rycroft, D.W., Williams, D.J.A., and Ingram, H.A.P. 1975. The transmission of water through peat: I.Review. *The journal of Ecology*, **63**(2): 535-556.
- Scott, R.C. 1989. Physical Geography. West Publishing, New York.
- Strahler, A.N. 1952b. Dynamic basis of Geomorphology. *Geologic Society of America Bulletin*, **63**: 923-938.
- Tarboton, D.G., Bras, R.L., and Rodriguez-Iturbe, I. 1988. The fractal nature of river networks. *Water Resource Research*, **24**(8): 1317-1322.
- Tarr, R.S., and Martin, L. 1914. *College Physiography*. Macmillian, New York.
- van Everdingen, R.O. 1976. Geocryological terminology. *Canadian Journal of Earth Sciences*, **13** (6): 862-867.
- Vardy, S.R., Warner, B.G., and Aravena, R. 1997. Holocene Climate Effects on the Development of a Peatland on the Tuktoyaktuk Peninsula, Northwest Territories. *Quaternary Research*, **47**: 90-104.
- Vorosmarty, C.J., Fekete, B.M., Meybeck, M., and Lammers, R.B. 2000. Geomorphometric attributes of the global system of rivers at 30-minute spatial resolution. *Journal of Hydrology*, **237**: 17-39.
- White, J.M., Ager, T.A., Adam, D.P., Leopold, E.B., Liu, G., and Jette, H. 1997. An 18 million year record of vegetation and climate change in northwestern Canada and Alaska;

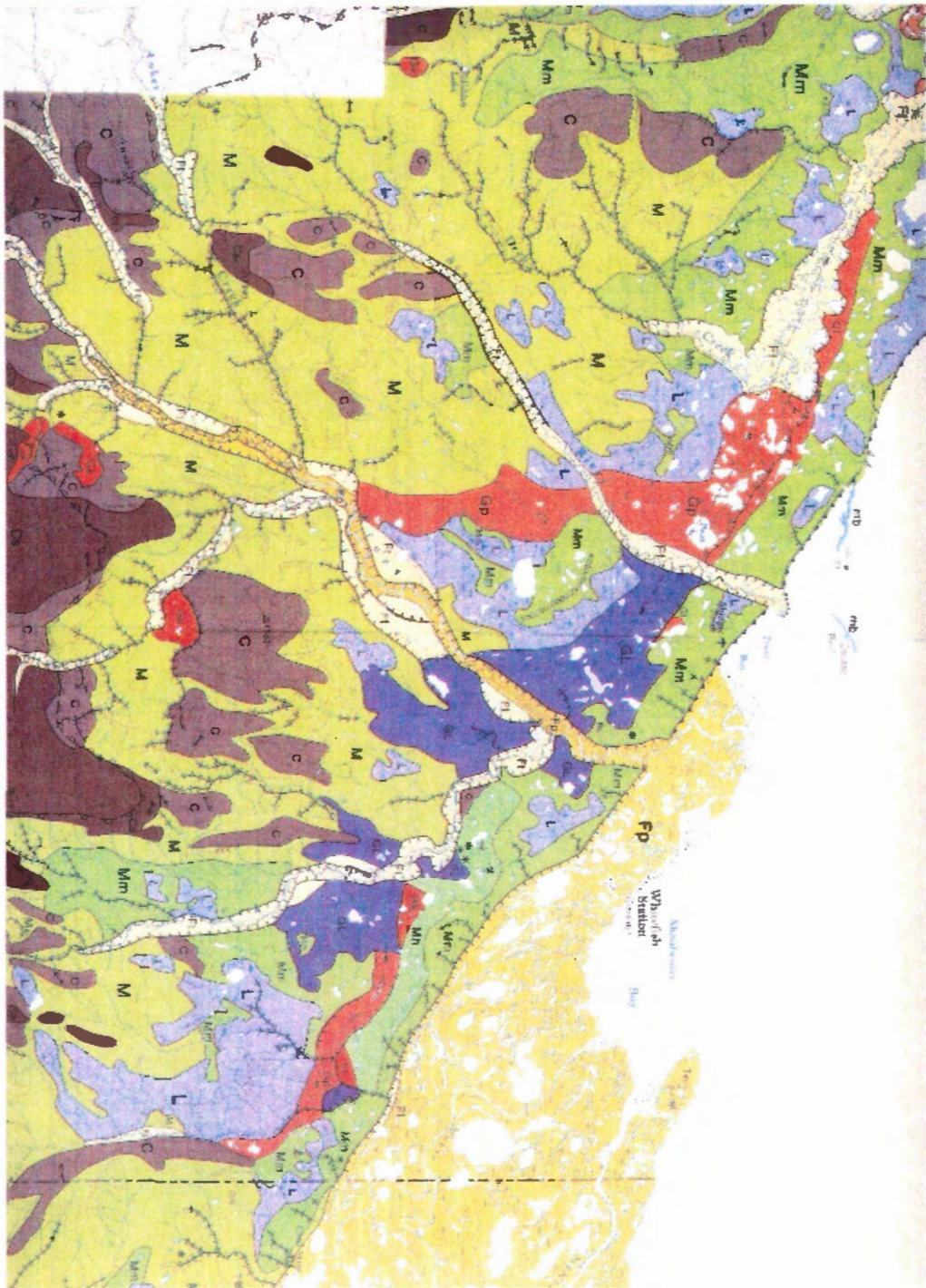
tectonic and global climatic correlates. *Palaeogeography, Palaeoclimatology, Palaeoecology*, **130**(1-4): 293-306.

Williams, P.J., and Smith, M.W. 1989. *The frozen earth: Fundamentals of geocryology*. Cambridge University Press, New York.

Woo, M.K., and Sauriol, J. 1981. Effects of snow jams on fluvial activities in the high Arctic. *Physical Geography*, **2**: 83-98.

Appendices A - E

Appendix A: Quaternary Geology of the Yukon Coastal Plain



QUATERNARY

POSTGLACIAL

mb	Marine beach, bar, or spit	Modern
Fp	Floodplain or valley plain	
Ftp	Low terrace or floodplain, undifferentiated	
Ft	Stream terrace	
Ff	Alluvial fan	
L	Lacustrine plain	

BUCKLAND GLACIATION (EARLY WISCONSIN ?)

GL	Glacial limit line	
Gl	Outwash fan	Includes late Wisconsin deposits adjacent to Mackenzie Upland near Atkasit
Gp	Outwash plain or valley plain	
Gf	Stream terrace or step	
M	Ground moraine	
Mm	Rolling moraine	
Mh	Hummocky moraine	
Mt	Ice-thrust moraine ridge	

PRE-BUCKLAND

Fd	Alluvial fan or deposit
UNDIFFERENTIATED	
C	Colluvial slope; gentle to moderate
Ca	Cliff or steep colluvial slope

Geological boundary
Glacial limit
Esker (direction of flow known)
Kame
Marine beach, bar, or spit
Maximum extent of glaciation (determined, approximate)
Canyon or steep-walled narrow valley, stream eroded
Canyon or steep-walled narrow valley, meltwater eroded
Direction of glacial meltwater flow in broad channel
Stream-cut escarpment
Coastal bluff or escarpment
Retrogressive mass flow slide

Geology by V.N. Rempton, 1970-72, 1976-78

To accompany Bulletin 317 by V.N. Rempton

Geological cartography by S.J. Frahmberg, Geological Survey of Canada

Any revisions or additional geological information known to the user would be welcomed by the Geological Survey of Canada

Base map assembled by the Geological Survey of Canada from maps published at the same scale in 1962, 1963, 1964, 1974

Mean magnetic declination 1975, 37°13' East, decreasing 1.9' annually. Readings vary from 35°46' in the NW corner to 38°10' in the SE corner of the map area

Elevations in feet above mean sea level

Appendix B: Digital Elevation Model MetaData

DEM	Reference Mapsheet(s) Code	Latitude/Longitude Range (degrees)	Horizontal Resolution (m)	Vertical Resolution (m)
yukonmerge_DEM	117 A, 117 C, 117 D	North edge: 70.000416666667 South edge: 67.999583333333 West edge: -142.000833333333 East edge: -135.999166666667	90	2.3
selected_area_DEM	N/A	North edge: 69.089583333333 South edge: 68.716250000000 West edge: -137.754166666666 East edge: -139.974166666666	90	2.3

DEM	Reference Mapsheet(s) Code	Latitude/Longitude Range (degrees)	Horizontal Resolution (m)	Vertical Resolution (m)
peacerivermerge_DE M	084 E, 084 F, 084K, 084L	North edge: 59.000416666667 South edge: 56.999583333333 West edge: -120.000416666667 East edge: -115.999583333333	90	2.3
selected_area_DEM	N/A	North edge: 58.044583333333 South edge: 57.614583333333 West edge: -117.755416666667 East edge: -117.055416666667	90	2.3

DEM	Reference Mapsheet(s) Code	Latitude/ Longitude Range (degrees)	Horizontal Resolution (m)	Vertical Resolution (m)
okanoganmerge_DE M	082 E, 082 L	North edge: 51.000416666667 South edge: 48.999583333333 West edge: -120.000416666667 East edge: -117.999583333333	90	2.3
selected_area_DEM	N/A	North edge: 50.249583333333 South edge: 49.817083333333 West edge: -119.432916666667 East edge: -119.010416666667	90	2.3

DEM	Reference Mapsheet(s) Code	Latitude/Longitude Range (degrees)	Horizontal Resolution (m)	Vertical Resolution (m)
novascotiamerge_DE M	011 D, 011E	North edge: 46.000416666667 South edge: 43.999583333333 West edge: -64.000416666667 East edge: -61.999583333333	90	2.3
selected_area_DEM	N/A	North edge: 45.244583333333 South edge: 44.912083333333 West edge: -62.277916666667 East edge: -62.012916666667	90	2.3

Appendix C: Aerial Photographs and Attributes

Photo	Item ID	Roll Number	Photo Number	Photo Date	Center Lat/Long	Scale
Yukon Coastal Plain	2444011	A13751	33	07/27/53	68.906085/ -137.286364	20000
Yukon Coastal Plain	2444000	A24124	99	07/15/75	68.608168/ -137.405059	60000
Yukon Coastal Plain	2441231	A26780	11	08/08/85	68.922613/ -137.291837	30000
Yukon Coastal Plain	2441233	A26780	13	08/08/85	68.944002/ -137.427281	30000
Yukon Coastal Plain	2441235	A26780	15	08/08/85	68.965863/ -137.562976	30000

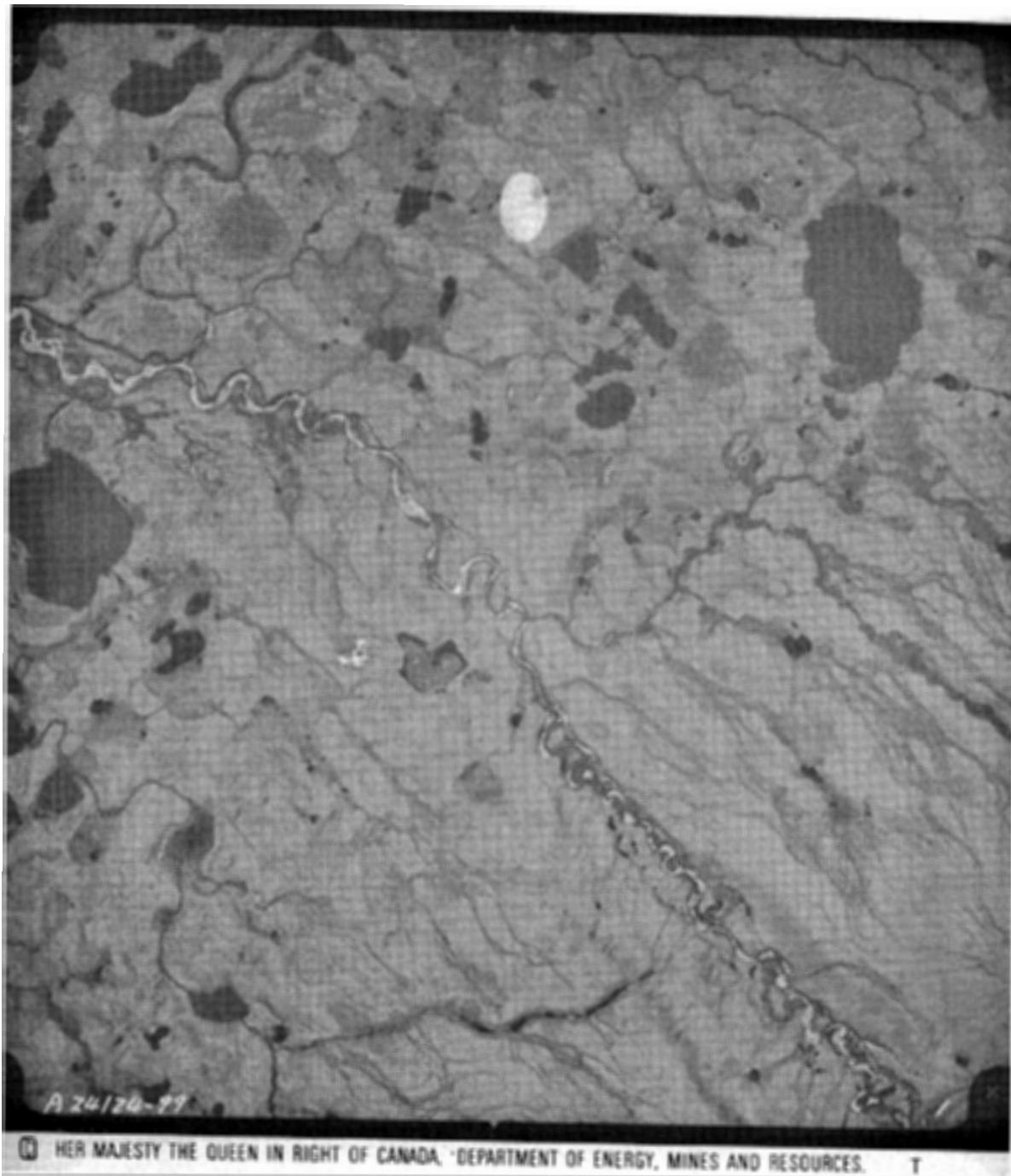
Aerial Photographs

© SA MAJESTE LA REINE DU CHEF DU CANADA, MINISTERE DE L'ENERGIE, DES MINES ET DES RESSOURCES.

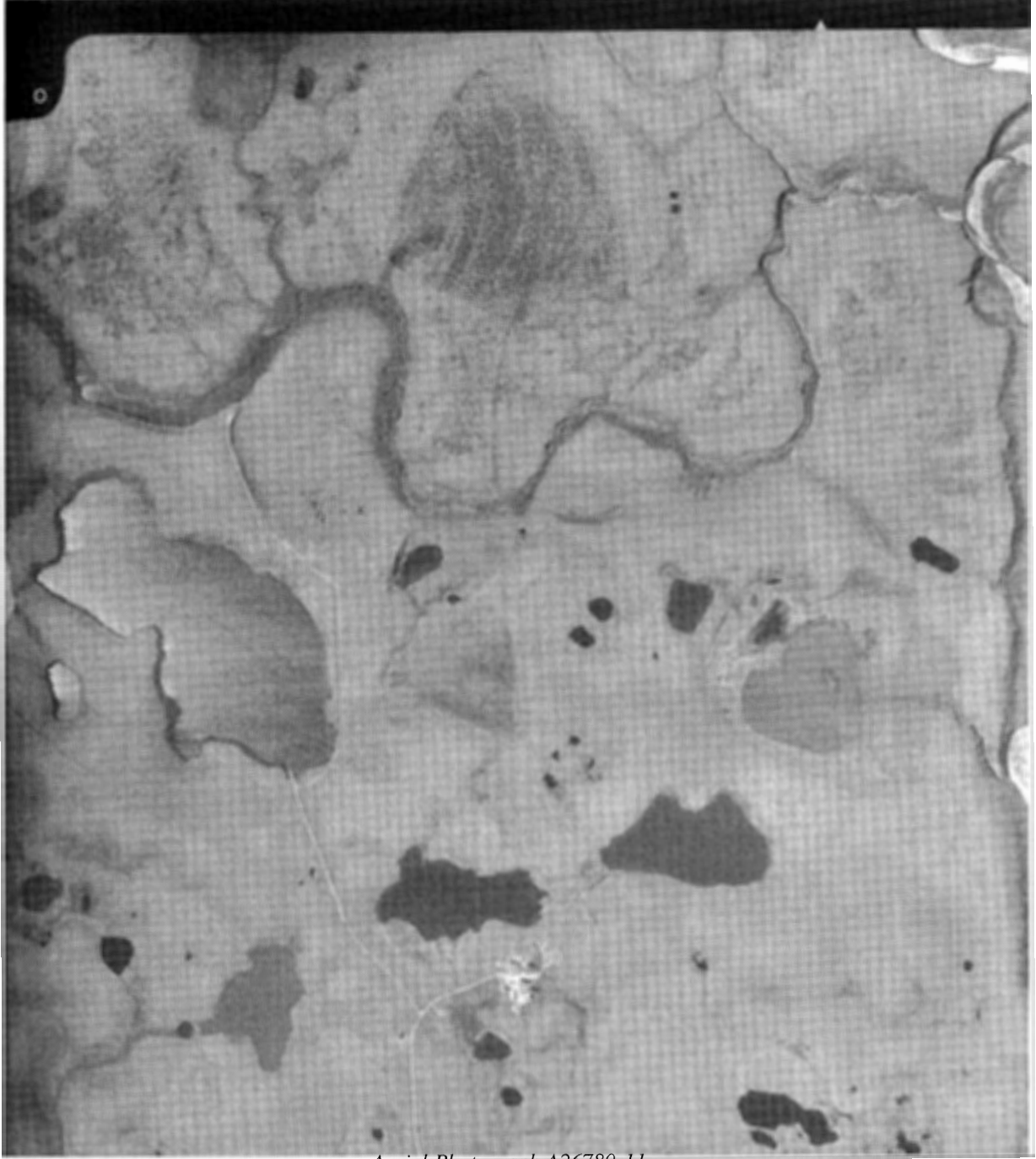


© HER MAJESTY THE QUEEN IN RIGHT OF CANADA, DEPARTMENT OF ENERGY, MINES AND RESOURCES.

Aerial photograph A13751-33

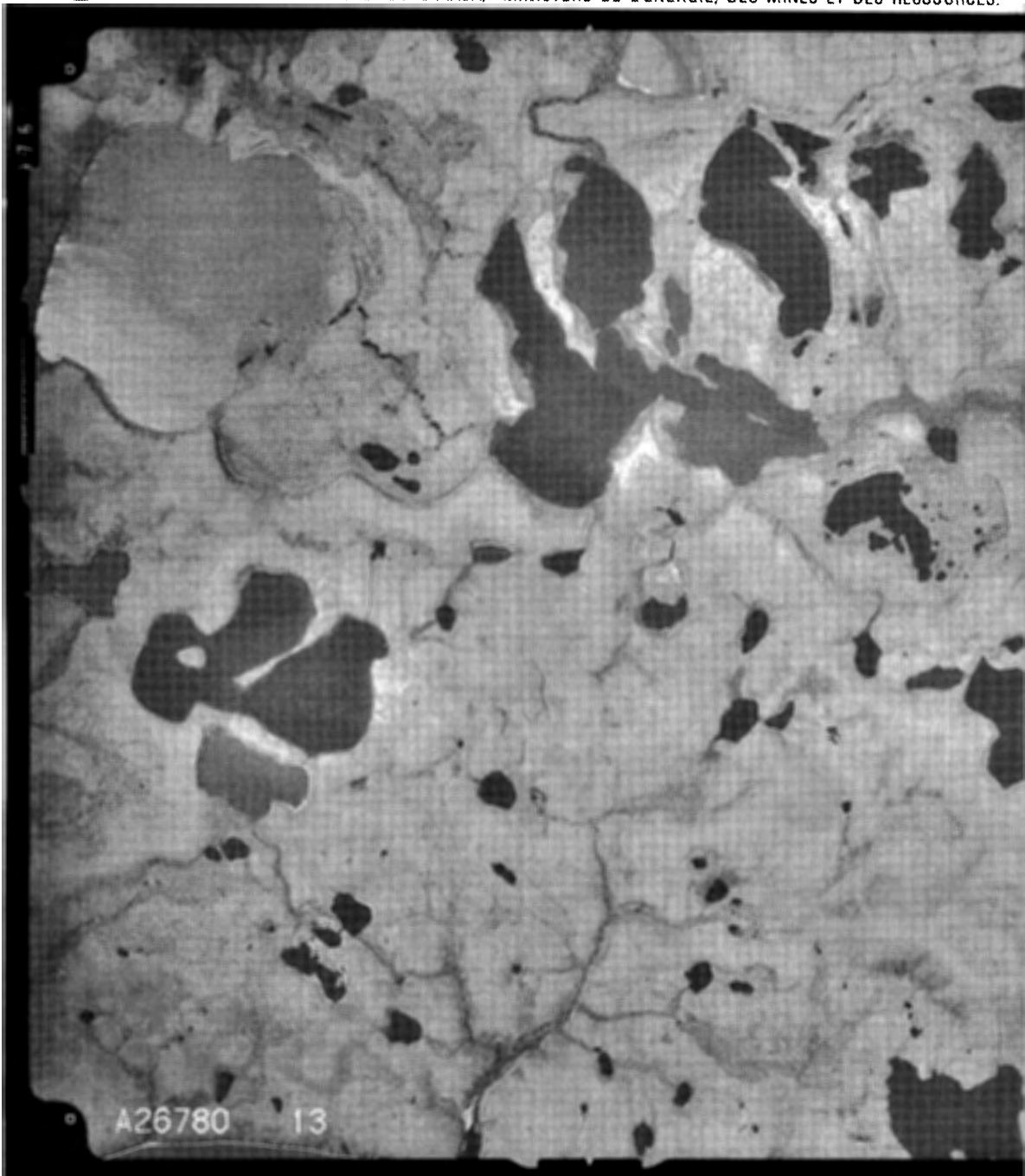


Aerial photograph A24124-99



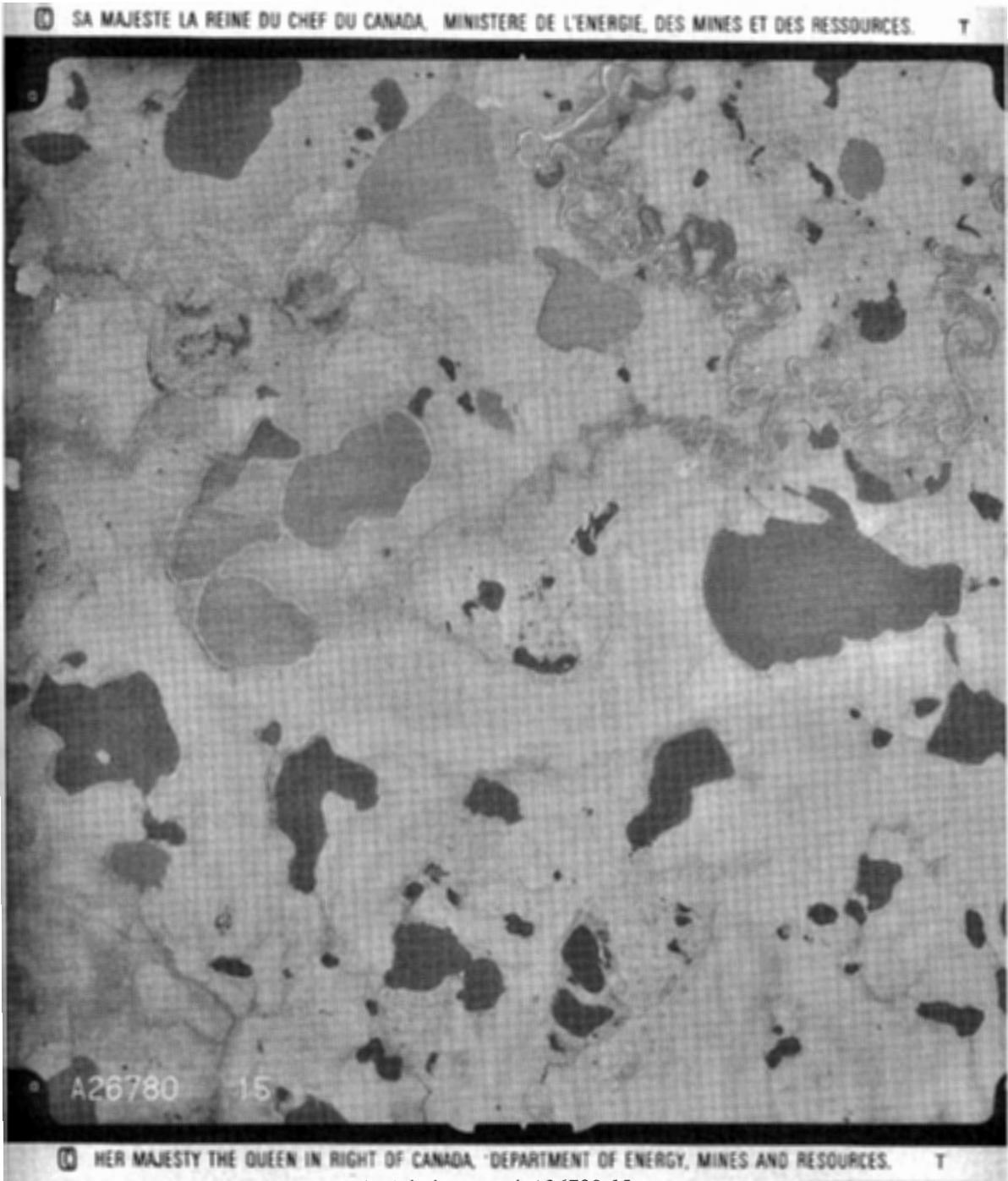
Aerial Photograph A26780-11

© SA MAJESTE LA REINE DU CHEF DU CANADA, MINISTERE DE L'ENERGIE, DES MINES ET DES RESSOURCES.



© HER MAJESTY THE QUEEN IN RIGHT OF CANADA, DEPARTMENT OF ENERGY, MINES AND RESOURCES.

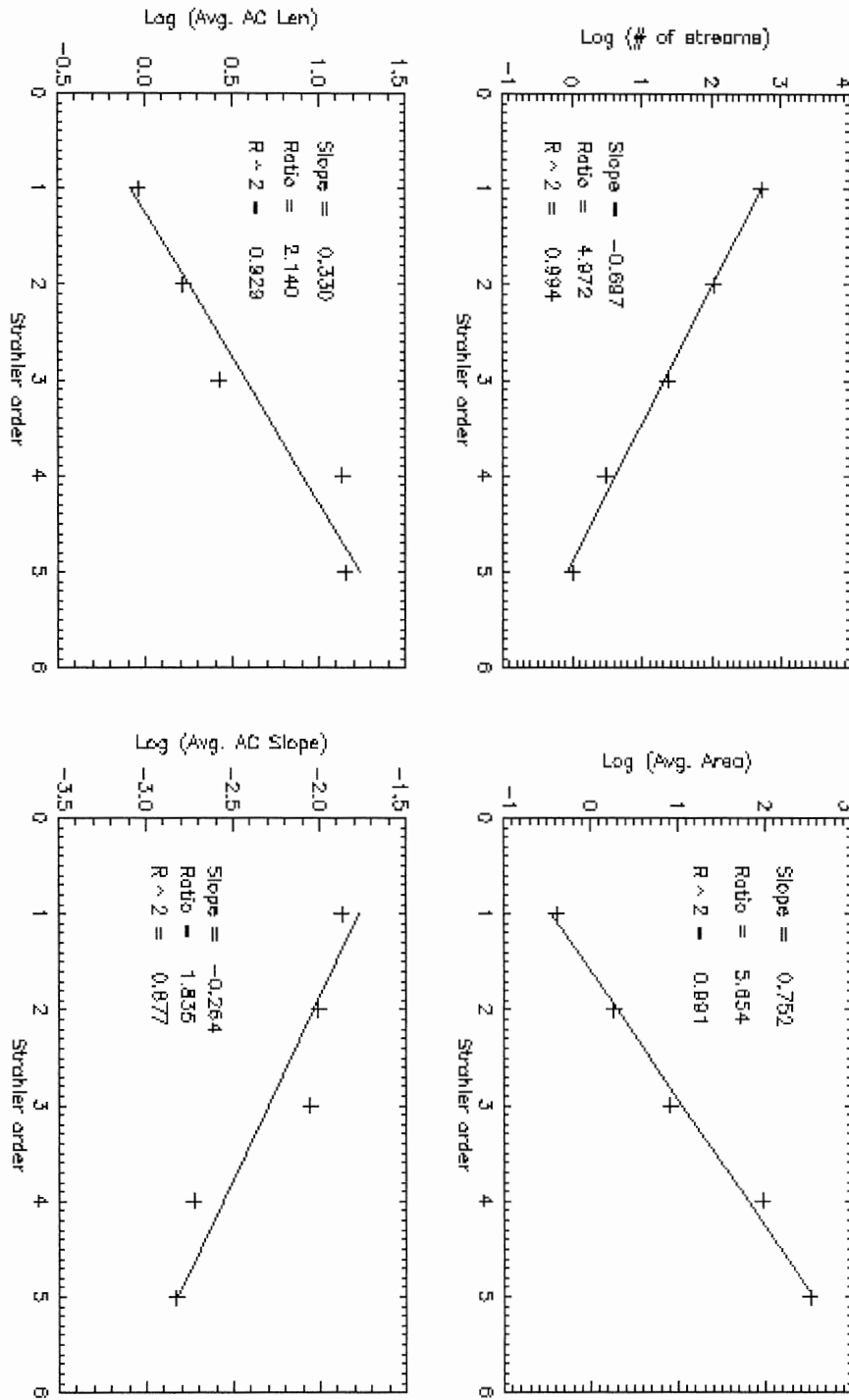
Aerial photograph A26780-13



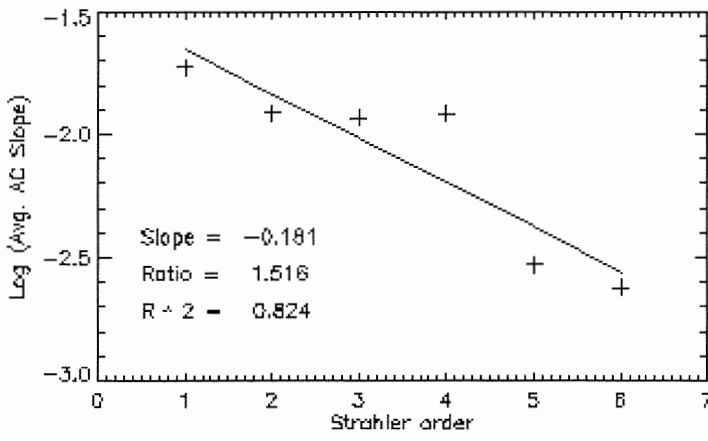
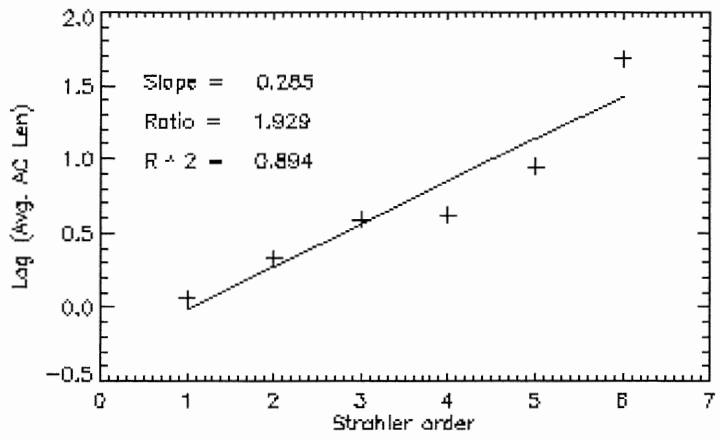
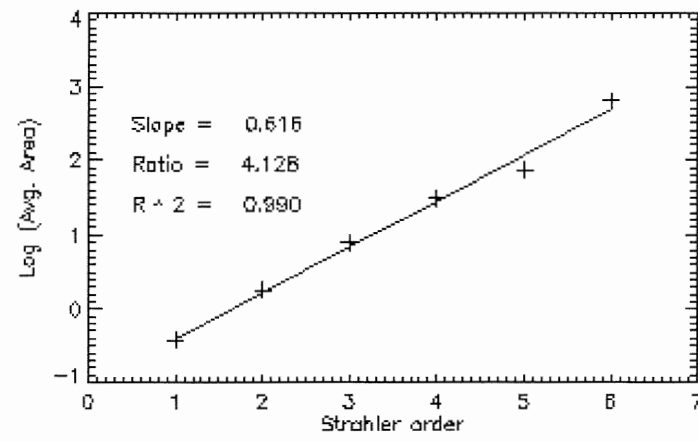
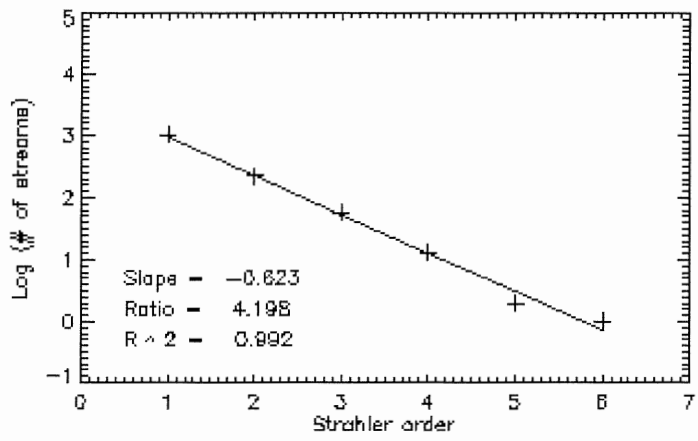
Aerial photograph A26780-15

Appendix D: Horton Plots for all Study Areas

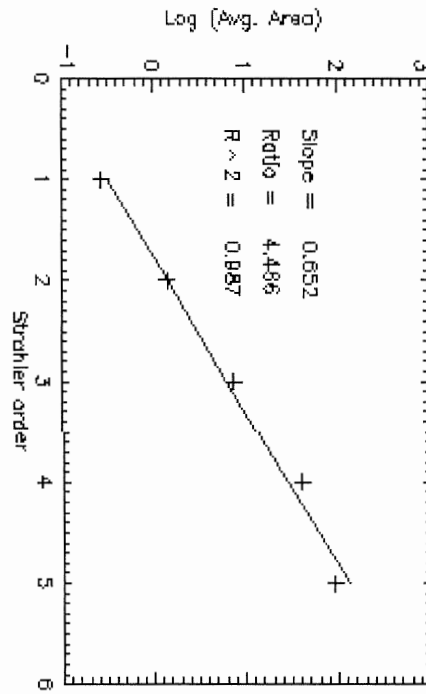
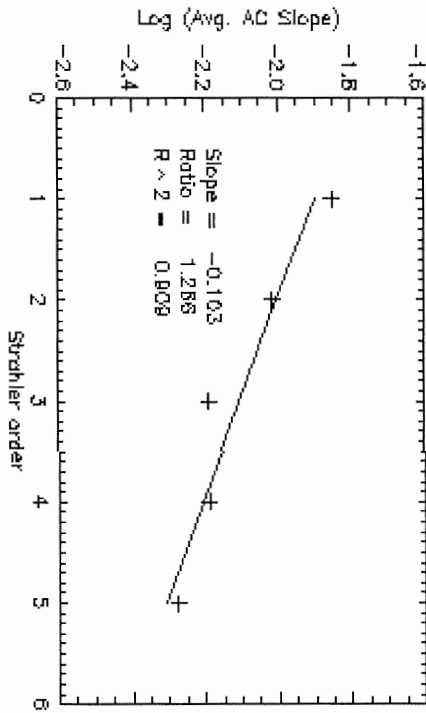
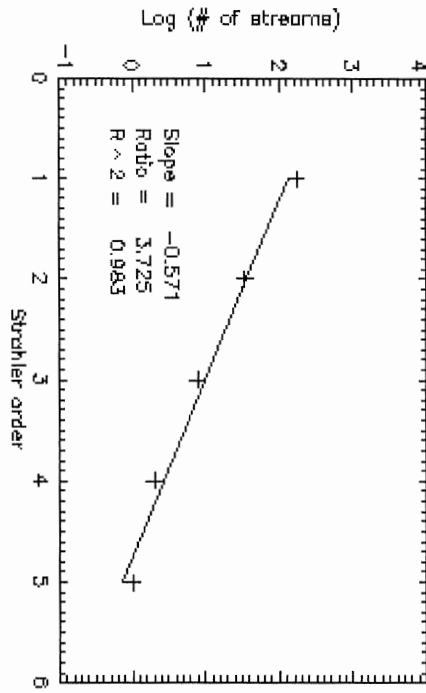
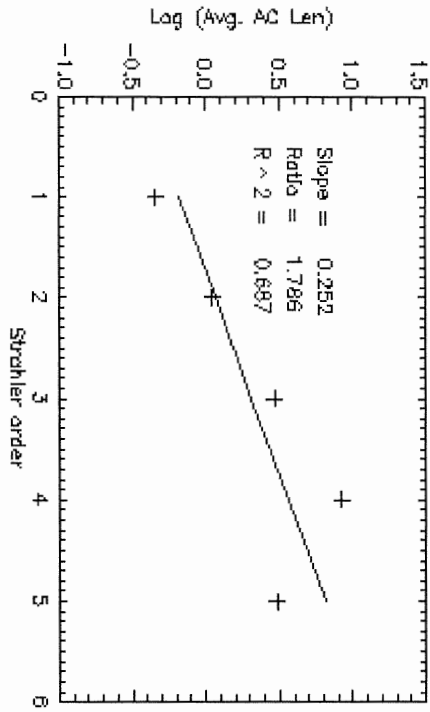
Running River, Yukon Territories



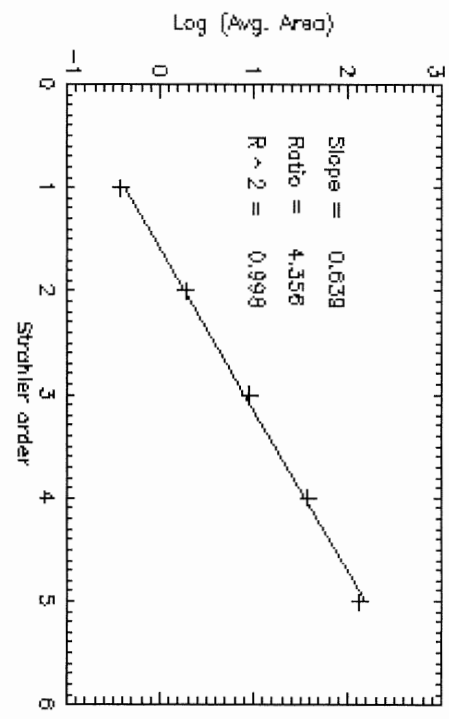
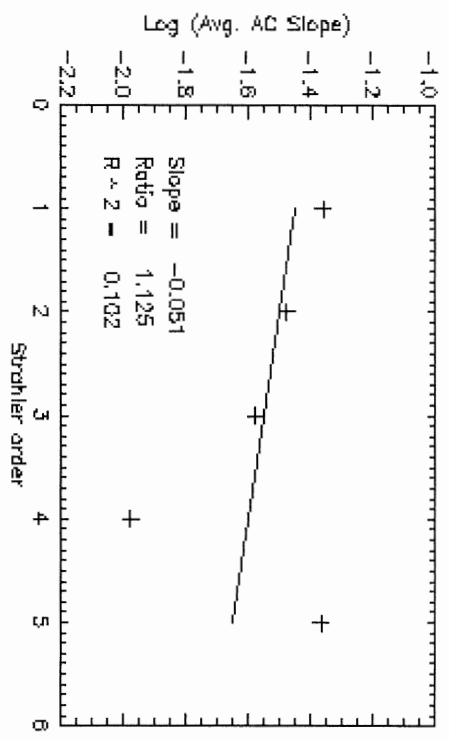
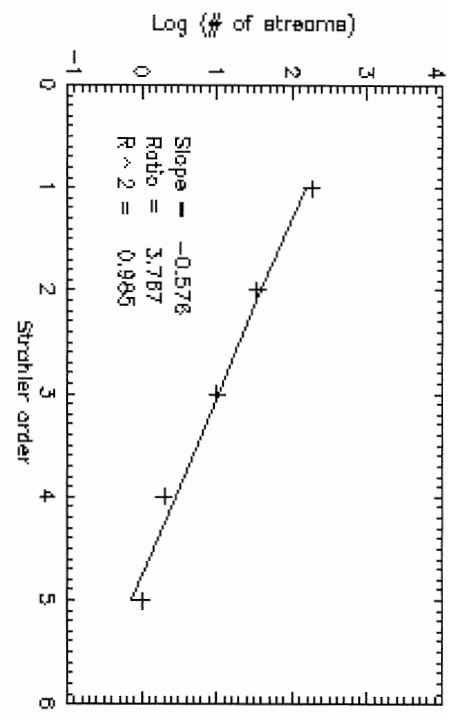
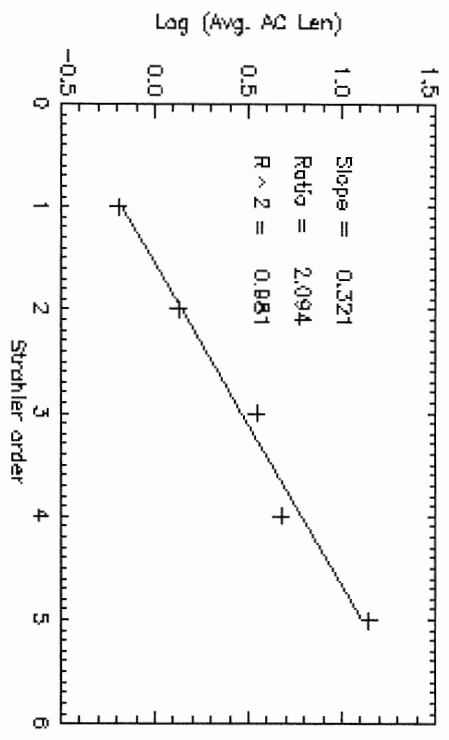
Keg River, Alberta



East River, Nova Scotia



Nicklen Creek, British Columbia



Appendix E: Calculations

Water Track and Open Water Channel Critical basin Area Calculations

1.0 Water Tracks

Water track at x:-137.29000
y: 68.905833

DATA SUMMARY FOR patched River BASIN

Prune type = Order, Threshold = 1.00000

		BASIN AREA				(km)^2	
Order	Number	Minimum	Maximum	Range	StdDev.	Average	
1	2	6.22742E-003	6.22765E-003	2.34228E-007	1.17114E-007	6.22754E-003	
2	1	1.86825E-002	1.86825E-002	0.00000E+000	0.00000E+000	1.86825E-002	

Water track at x:-137.31667
y: 68.808333

DATA SUMMARY FOR patched River BASIN

Prune type = Order, Threshold = 1.00000

		BASIN AREA				(km)^2	
Order	Number	Minimum	Maximum	Range	StdDev.	Average	
1	6	6.25407E-003	6.25594E-003	1.87010E-006	6.03571E-007	6.25524E-003	
2	1	1.12585E-001	1.12585E-001	0.00000E+000	0.00000E+000	1.12585E-001	

water tracks at x:-137.33500
y: 68.798333

DATA SUMMARY FOR patched River BASIN

Prune type = Order, Threshold = 0.000000

		BASIN AREA				(km)^2	
Order	Number	Minimum	Maximum	Range	StdDev.	Average	
1	1	1.87685E-002	1.87685E-002	0.00000E+000	0.00000E+000	1.87685E-002	

water track at x:-137.37500
y: 68.772500

 DATA SUMMARY FOR patched River BASIN

Prune type = Order, Threshold = 2.00000

BASIN AREA							(km)^2
Order	Number	Minimum	Maximum	Range	StdDev.	Average	
1	2	7.51648E-002	1.19007E-001	4.38425E-002	2.19213E-002	9.70861E-002	
2	1	2.12959E-001	2.12959E-001	0.00000E+000	0.00000E+000	2.12959E-001	

water track at x:-137.39000
 y: 68.767500

 DATA SUMMARY FOR patched River BASIN

Prune type = Order, Threshold = 1.00000

BASIN AREA							(km)^2
Order	Number	Minimum	Maximum	Range	StdDev.	Average	
1	2	6.25992E-003	6.26015E-003	2.33762E-007	1.16881E-007	6.26003E-003	
2	1	1.87800E-002	1.87800E-002	0.00000E+000	0.00000E+000	1.87800E-002	

water track at x:-137.39833
 y: 68.762500

 DATA SUMMARY FOR patched River BASIN

Prune type = Order, Threshold = 1.00000

BASIN AREA							(km)^2
Order	Number	Minimum	Maximum	Range	StdDev.	Average	
1	7	6.26669E-003	1.87987E-002	1.25320E-002	4.38504E-003	1.43225E-002	
2	1	1.37855E-001	1.37855E-001	0.00000E+000	0.00000E+000	1.37855E-001	

water track at x:-137.43000
 y: 68.755000

 DATA SUMMARY FOR patched River BASIN

Prune type = Order, Threshold = 1.00000

BASIN AREA							(km)^2
Order	Number	Minimum	Maximum	Range	StdDev.	Average	
1	7	6.26669E-003	1.88022E-002	1.25355E-002	4.38612E-003	1.43248E-002	
2	1	2.00551E-001	2.00551E-001	0.00000E+000	0.00000E+000	2.00551E-001	

water track at x:-137.53333

y: 68.729167

DATA SUMMARY FOR patched River BASIN

Prune type = Order, Threshold = 2.00000

		BASIN AREA			(km)^2	
Order	Number	Minimum	Maximum	Range	StdDev.	Average
1	2	5.02022E-002	1.00409E-001	5.02069E-002	2.51034E-002	7.53057E-002
2	1	1.94534E-001	1.94534E-001	0.00000E+000	0.00000E+000	1.94534E-001

water track at x:-137.56167
y: 68.729167

DATA SUMMARY FOR patched River BASIN

Prune type = Order, Threshold = 2.00000

		BASIN AREA			(km)^2	
Order	Number	Minimum	Maximum	Range	StdDev.	Average
1	2	5.64815E-002	6.90320E-002	1.25504E-002	6.27522E-003	6.27567E-002
2	1	1.44338E-001	1.44338E-001	0.00000E+000	0.00000E+000	1.44338E-001

water track at x:-137.73000
y: 68.729167

DATA SUMMARY FOR patched River BASIN

Prune type = Order, Threshold = 0.000000

		BASIN AREA			(km)^2	
Order	Number	Minimum	Maximum	Range	StdDev.	Average
1	1	1.88281E-002	1.88281E-002	0.00000E+000	0.00000E+000	1.88281E-002

water track at x:-137.72333
y: 68.735000

DATA SUMMARY FOR patched River BASIN

Prune type = Order, Threshold = 0.000000

		BASIN AREA			(km)^2	
Order	Number	Minimum	Maximum	Range	StdDev.	Average
1	1	5.01915E-002	5.01915E-002	0.00000E+000	0.00000E+000	5.01915E-002

water track at x:-137.70000
y: 68.777500

DATA SUMMARY FOR patched River BASIN

Prune type = Order, Threshold = 1.00000

		BASIN AREA			(km)^2	
Order	Number	Minimum	Maximum	Range	StdDev.	Average
1	4	1.25231E-002	7.51468E-002	6.26237E-002	2.48036E-002	3.28758E-002
2	1	1.50288E-001	1.50288E-001	0.00000E+000	0.00000E+000	1.50288E-001

water track at x:-137.72500
y: 68.821667

DATA SUMMARY FOR patched River BASIN

Prune type = Order, Threshold = 2.00000

		BASIN AREA			(km)^2	
Order	Number	Minimum	Maximum	Range	StdDev.	Average
1	2	3.12442E-002	5.62359E-002	2.49918E-002	1.24959E-002	4.37401E-002
2	1	1.24973E-001	1.24973E-001	0.00000E+000	0.00000E+000	1.24973E-001

water track at x:-137.64500
y: 68.828333

DATA SUMMARY FOR patched River BASIN

Prune type = Order, Threshold = 0.000000

		BASIN AREA			(km)^2	
Order	Number	Minimum	Maximum	Range	StdDev.	Average
1	1	1.87440E-002	1.87440E-002	0.00000E+000	0.00000E+000	1.87440E-002

water track at x:-137.55333
y: 68.858333

DATA SUMMARY FOR patched River BASIN

Prune type = Order, Threshold = 2.00000

		BASIN AREA			(km)^2	
Order	Number	Minimum	Maximum	Range	StdDev.	Average
1	3	5.61462E-002	1.68461E-001	1.12315E-001	5.29453E-002	9.35854E-002
2	1	2.93233E-001	2.93233E-001	0.00000E+000	0.00000E+000	2.93233E-001

water track at x:-137.56500
y: 68.865000

DATA SUMMARY FOR patched River BASIN

Prune type = Order, Threshold = 0.000000

		BASIN AREA			(km)^2	
Order	Number	Minimum	Maximum	Range	StdDev.	Average
1	1	6.23654E-003	6.23654E-003	0.00000E+000	0.00000E+000	6.23654E-003

water track at x:-137.38833
y: 68.899167

DATA SUMMARY FOR patched River BASIN

Prune type = Order, Threshold = 1.00000

		BASIN AREA			(km)^2	
Order	Number	Minimum	Maximum	Range	StdDev.	Average
1	2	6.22742E-003	1.86830E-002	1.24555E-002	6.22777E-003	1.24552E-002
2	1	3.11376E-002	3.11376E-002	0.00000E+000	0.00000E+000	3.11376E-002

water track at x:-137.49500
y: 68.912500

DATA SUMMARY FOR patched River BASIN

Prune type = Order, Threshold = 1.00000

		BASIN AREA			(km)^2	
Order	Number	Minimum	Maximum	Range	StdDev.	Average
1	6	1.24455E-002	1.86696E-002	6.22415E-003	2.93381E-003	1.45206E-002
2	1	2.05367E-001	2.05367E-001	0.00000E+000	0.00000E+000	2.05367E-001

water track at x:-137.52500
y: 68.964167

DATA SUMMARY FOR patched River BASIN

Prune type = Order, Threshold = 1.00000

		BASIN AREA			(km)^2	
Order	Number	Minimum	Maximum	Range	StdDev.	Average
1	3	6.20824E-003	1.24160E-002	6.20777E-003	2.92631E-003	8.27757E-003

2 1 4.34577E-002 4.34577E-002 0.00000E+000 0.00000E+000 4.34577E-002

water track at x:-137.37167
y: 68.930000

DATA SUMMARY FOR patched River BASIN

Prune type = Order, Threshold = 2.00000

		BASIN AREA			(km)^2	
Order	Number	Minimum	Maximum	Range	StdDev.	Average
1	2	3.10913E-002	4.35285E-002	1.24373E-002	6.21865E-003	3.73099E-002
2	1	8.70571E-002	8.70571E-002	0.00000E+000	0.00000E+000	8.70571E-002

Critical Basin Area Mean of 20 chosen water tracks: 0.1044 km²

Critical Basin Area Standard Deviation of 20 chosen water tracks: 0.0855 km²

2.0 Open Water Channels

Running River, NT

open water channel at x:-137.55833
y: 68.773333

DATA SUMMARY FOR patched River BASIN

Prune type = Order, Threshold = 0.000000

		BASIN AREA			(km)^2	
Order	Number	Minimum	Maximum	Range	StdDev.	Average
1	1	6.26272E-003	6.26272E-003	0.00000E+000	0.00000E+000	6.26272E-003

open water channel at x:-137.51333
y: 68.945833

DATA SUMMARY FOR patched River BASIN

Prune type = Order, Threshold = 3.00000

		BASIN AREA			(km)^2	
Order	Number	Minimum	Maximum	Range	StdDev.	Average
1	1	1.50047E+001	1.50047E+001	0.00000E+000	0.00000E+000	1.50047E+001

open water channel at x:-137.66600
y: 68.804167

DATA SUMMARY FOR patched River BASIN

Prune type = Order, Threshold = 3.00000

		BASIN AREA			(km)^2	
Order	Number	Minimum	Maximum	Range	StdDev.	Average
1	1	1.80732E+001	1.80732E+001	0.00000E+000	0.00000E+000	1.80732E+001

Mean Critical Area of Running River: 11.0281 km²

Standard Deviation of Running River: 9.6677 km²

Vertical Resolution Calculations:

GPS Elevation (m) (Gardner 2005)			DEM Elevation (m)			Vertical Resolution (m)
Elevation 1	Elevation 2	Δ Elevation	Elevation 1	Elevation 2	Δ Elevation	ABS[Δ GPS - Δ DEM]
38.5427	35.2257	3.317	18.0	16.0	2.0	1.317
36.2502	34.2548	1.995	16.0	17.0	1.0	0.995
36.6381	34.9870	1.651	15.0	12.0	3.0	1.349
35.2257	35.0411	0.185	16.0	12.0	4.0	3.815
39.0463	36.5350	2.511	18.0	12.0	6.0	3.489
36.2302	34.9870	1.243	16.0	12.0	4.00	2.757
35.2257	31.3306	3.895	16.0	18.0	2.00	1.895
38.5427	34.9870	3.556	18.0	12.0	6.00	2.444
36.5350	35.2257	1.309	12	16	4.00	2.691
39.0463	35.0411	4.005	18	12	6.0	1.995

Mean Vertical resolution for Study Site: 2.2747 m
Standard Deviation: 0.9378 m